

7-2019

# Topography Study of FIXa: Generation of a Lipid Anchored Molecular Ruler with Attached Inhibitor

Nickolas P. Buchanan

*Philadelphia College of Osteopathic Medicine*

Follow this and additional works at: <https://digitalcommons.pcom.edu/biomed>

 Part of the [Medicine and Health Sciences Commons](#)

---

## Recommended Citation

Buchanan, Nickolas P., "Topography Study of FIXa: Generation of a Lipid Anchored Molecular Ruler with Attached Inhibitor" (2019). *PCOM Biomedical Studies Student Scholarship*. 159.  
<https://digitalcommons.pcom.edu/biomed/159>

This Thesis is brought to you for free and open access by the Student Dissertations, Theses and Papers at DigitalCommons@PCOM. It has been accepted for inclusion in PCOM Biomedical Studies Student Scholarship by an authorized administrator of DigitalCommons@PCOM. For more information, please contact [library@pcom.edu](mailto:library@pcom.edu).

**Philadelphia College of Osteopathic Medicine - Georgia Campus**

**Biomedical Sciences Master Program**

**Department of Biomedical Sciences**

**TOPOGRAPHY STUDY OF FIXA:  
GENERATION OF A LIPID ANCHORED MOLECULAR RULER  
WITH ATTACHED INHIBITOR**

A Thesis in Biomedical Research by Nickolas P. Buchanan  
Advisor: Kimberly J. Baker, Ph.D.

Copyright 2019 Nickolas P. Buchanan

Submitted in Partial Fulfillment of the Requirements for the Degree of  
Master of Science in Biomedical Sciences

July, 2019

## Signatory Page for Master's Thesis

We approve the thesis of Nickolas P. Buchanan.

\_\_\_\_\_ Date \_\_\_\_\_

Kimberly Baker  
Associate Professor of Biochemistry  
Thesis Advisor

\_\_\_\_\_ Date \_\_\_\_\_

Francis E. Jenney, Jr.  
Associate Professor of Biochemistry  
Committee Member

\_\_\_\_\_ Date \_\_\_\_\_

Shu Zhu  
Associate Professor of Neuroscience, Physiology and Pharmacology  
Committee Member

\_\_\_\_\_ Date \_\_\_\_\_

Richard E. White  
Associate Director, Biomedical Sciences  
Professor of Neuroscience, Physiology and Pharmacology

# TOPOGRAPHY STUDY OF FIXA: GENERATION OF A LIPID ANCHORED MOLECULAR RULER WITH ATTACHED INHIBITOR

## Abstract

Blood coagulation, an important hemostatic property, is directed through activation of proteolytic enzymes known as serine proteases to generate a fibrin plug. Using multiple proteases allows for localized and precise regulation of blood coagulation within the circulatory system. Factor IX, a serine protease, is a key activator in the coagulation cascade by activating Factor X. For activation of FX to occur, FIXa must be in proper conformation on the platelet surface with cofactor FVIIIa to increase enzymatic abilities of FIXa a billion-fold. Current research looks at structure and function of FIXa yet neglects structural plasticity on the membrane, with function of FIX clearly being related to conformation on the platelet. The role of this investigation was to study the optimal reactive topography of FIXa by generating AMRI, Aadjustable height Molecular Ruler with attached Inhibitor. AMRI composed of three primary regions contains an Anchor region, Linker region, and Inhibitor. AMRI was generated using the protein anchoring sequence LAGC to fixate to a lipid surface. A height adjustable linker area was then required between the anchor and inhibitor regions of AMRI to ensure proper vertical height of inhibitor. The linker sequence EAAAK forms a rigid structure with a vertical height of 7.5Å above the membrane surface, thus we repeated this sequence to achieve a specific desired height. Completing the

protein's linker region is a flexible linker at end of the rigid set. That flexible linker ensures the inhibitor will fit in FIXa active site. Finishing the AMRI complex is a PN2-KPI inhibitor, which has been demonstrated to fit and inhibit the catalytic site of FIXa. Therefore, AMRI should allow for determination of optimal reactive height of the FIXa active site without affecting structural conformation. Through the generation of AMRI, a greater insight into blood coagulation will be gained, along with potential for site specific anticoagulant clinical applications.

# TABLE OF CONTENTS

<b>LIST OF FIGURES .....</b>	<b>VI</b>
<b>LIST OF TABLES .....</b>	<b>VII</b>
<b>LIST OF ABBREVIATIONS.....</b>	<b>VIII</b>
<b>ACKNOWLEDGMENTS .....</b>	<b>X</b>
<b>1 BACKGROUND AND SIGNIFICANCE.....</b>	<b>1</b>
1.1 HEMOSTASIS .....	1
1.2 PLATELET ACTIVATION AND COAGULATION CASCADE .....	2
1.3 SERINE PROTEASES.....	9
1.4 FACTOR IX.....	14
1.5 ANTI-COAGULATION AND INHIBITOR STRUCTURE .....	16
<b>2 RESEARCH DESIGN .....</b>	<b>18</b>
2.1 PROTEASE NEXIN2 - KUNITZ PROTEASE INHIBITOR (PN2-KPI).....	20
2.2 LAGC ANCHOR WITH APYRASE LEADER SEQUENCE .....	21
2.3 LINKERS= (EAAAK) <sub>11</sub> (GGGGS).....	22
<b>4 SPECIFIC AIMS .....</b>	<b>24</b>
<b>5 METHODS .....</b>	<b>25</b>
5.1 SNAPGENE .....	25
5.2 VECTOR PREPARATION.....	25
5.3 DNA ANALYSIS .....	30
5.4 RESUSPENSION OF LYOPHILIZED PN2 OLIGONUCLEOTIDE .....	32
5.5 DESIGN OF PN2.....	32
5.6 RESTRICTION DIGEST .....	35

5.7	PURIFICATION .....	36
5.8	LIGATION.....	38
5.9	POLYMERASE CHAIN REACTION .....	38
5.10	DNA EXTRACTION FROM AGAROSE GELS.....	42
<b>6</b>	<b>RESULTS.....</b>	<b>44</b>
6.1	DISSECTION OF PET11D.....	44
6.2	PCR REORIENTATION AND PURIFICATION OF AMR .....	45
6.3	PURIFICATION OF RESTRICTED PET11D PLASMID.....	48
6.4	INSERTION AND TRANSFORMATION OF AMR INSERT .....	50
6.5	ANNEALING AND PURIFICATION OF PN2-KPI .....	51
6.6	HARVEST OF P_AMR FOR USE IN TRANSFORMATION .....	51
6.7	LIGATION AND TRANSFORMATION OF P-AMR WITH PN2-KPI .....	52
<b>7</b>	<b>DISCUSSION .....</b>	<b>54</b>
<b>8</b>	<b>FUTURE STUDIES.....</b>	<b>57</b>
8.1	PROTEIN EXPRESSION AND PURIFICATION OF AMRI .....	57
8.2	DETERMINE ABILITY OF AMRI TO INHIBIT FIXA.....	61
<b>9</b>	<b>CLINICAL SIGNIFICANCE.....</b>	<b>63</b>
	<b>REFERENCES.....</b>	<b>65</b>
<b>10</b>	<b>APPENDICES.....</b>	<b>73</b>
10.1	APPENDIX A. SEQUENCE DATA IMAGES OF AMR.....	73
10.2	APPENDIX B. SEQUENCE DATA IMAGES OF AMRI .....	78





## ***LIST OF FIGURES***

Figure 1 Platelet Adhesion Steps.....	4
Figure 2 Blood Coagulation Cascade.....	6
Figure 3 General Structure of Coagulation Factor.....	10
Figure 4 Structure of Factor IX.....	14
Figure 5 Demonstration of Coagulation Factor Knowledge.....	19
Figure 6 Linker Structure.....	23
Figure 7 pET-11d Vector Map.....	44
Figure 8 Vector Map of Inherited Sequence.....	45
Figure 9 Master Plan Diagram.....	47
Figure 10 Gel Confirmation of AMR PCR Product.....	48
Figure 11 Gel of pET-11d Restriction.....	49
Figure 12 Transformation of AMR.....	50
Figure 13 Gel Confirmation of AMR.....	50
Figure 14 Transformation of AMRI.....	52
Figure 15 Gel Confirmation of AMRI.....	52
Figure 16 Hypothesized Action of AMRI.....	54

***LIST OF TABLES***

Table 1 Blood Coagulation Proteins.....	5
---	---

## ***LIST OF ABBREVIATIONS***

Anchored Molecular Ruler with attached Inhibitor	AMRI
Activated Protein C	APC
Activated Protein S	APS
Amyloid $\beta$ Protein Precursor	A $\beta$ PP
Antithrombin III	AT
Bovine Pancreatic Trypsin Inhibitor	BPTI
Calf Intestinal Phosphatase	CIP
Cell-Based Model for Coagulation	CBMC
Glutamic Acid, (Alanine) <sub>3</sub> , Lysine	EAAAK
Epidermal Growth Factor	EGF
Factor I	FI
Factor II	FII
Factor III	FIII
Factor IV	FIV
Factor IX	FIX
Factor V	FV
Factor VI	FVI
Factor VII	FVII
Factor VIII	FVIII
Factor X	FX
Factor XI	FXI
Factor XII	FXII
Factor XIII	FXIII
Fluorescence Resonance Energy Transfer	FRET
Glycoprotein	GP
Kunitz Protease Inhibitor	KPI
Leucine Alanine Glycine Cysteine	LAGC
LAGC-(EAAAK) <sub>11</sub>	AMR
Plasminogen Activator	PA
Polymerase chain reaction	PCR
Phosphatidylcholine	PC
Phosphatidylserine	PS
Protease Nexin2	PN2
Protease Nexin2 - Kunitz Protease Inhibitor	PN2-KPI
Ribosome Binding Site	RBS
Single Chain Urokinase	SCU

Surface Plasmon Resonance	SPR
Tris-Acetate-EDTA Buffer	TAE Buffer
Tenase	Xase
Thrombomodulin	TM
Tissue Plasminogen Activator	tPA
von Willebrand Factor	vWF
Gamma-Carboxyglutamic Acid Domain	Gla

## **ACKNOWLEDGMENTS**

Firstly, I would love to express my eternal gratitude to my advisor, Dr. Kimberly Baker, for her support throughout my thesis research and writing. She enabled me to be able to explore life, question the boundaries, and challenged my understanding. Growth was the key to success, and I could not have asked for a better advisor to guide that growth.

Along with my advisor, I also wish to thank my committee members, Dr. Shu Zhu and Dr. Francis Jenney. Their insight was the perfect blend of support and encouragement to seek a great understanding of unknown scientific knowledge.

I wish to thank everyone in the Research Laboratory and Biomedical Sciences Department that provided amazing discussions. The friendships that developed at PCOM-GA over sleepless nights of studying and running experiments will last a lifetime.

Additionally, I would like to thank my family for supporting me throughout my life on all endeavors. Last and certainly not least, my boyfriend, Young, for the uncompromised support, understanding, and love through all I have put him through to achieve this goal.

# **1 Background and Significance**

## **1.1 Hemostasis**

Humans are dependent upon the circulation of blood through a pressurized vascular network to sustain life. Continuous blood flow is vital for the transport of nutrients, hormones, and waste to allow proper cellular function. The body includes five major vessel types christened arteries, arterioles, capillaries, venules, and veins. The arteries and veins contain three different layers termed the tunica intima, tunica media, and tunica adventitia; constructing the inner, middle, and outer layers, respectively. The arterioles and venules contain two layers, tunica intima, and tunica media. The capillaries contain only one layer, the tunica intima. The tunica intima is composed of a single layer of endothelial cells found in all blood vessels. The other two layers of the blood vessels are comprised of an extracellular matrix composed of collagens, elastins, fibrils, and proteoglycans, which provide structure and regulation to blood flow(1, 2).

Hemostasis is the balance of clotting at the site of injury, fibrinolysis as part of healing and preventing the random clotting to allow flow of blood throughout its system. The hemostatic system has the responsibility of maintaining integrity of the closed vascular system. Vascular integrity can be affected by a multitude of things including, a needle used to draw someone's blood, rupture of an atherosclerotic plaque, or a deep laceration during a motor vehicle accident. It is possible that one of these events or others could affect an individual at any given time, significantly affecting blood flow.

Failure of vascular integrity resulting in diminished hemostasis will lead to various clinical pathologies and in extreme circumstances, tissue, and cellular death(3).

## ***1.2 Platelet Activation and Coagulation Cascade***

The process of blood changing from a flowing liquid to forming a solid clot is coagulation. The ultimate goal of coagulation is to achieve hemostasis, by pinpointing and obstructing the loss of blood at the site of vascular injury. This happens with the activation and adhesion of platelets providing a surface for clotting enzymes to undergo a series of reactions forming a clot. These series of enzymatic reactions in conjunction with platelets can seal off the area of vascular damage by generation of a non-soluble plasma protein, fibrin(4-6) .

Platelets are found in significant numbers within the blood. In intact blood circulation, platelets are smooth, discoid in shape, and contain an internal canalicular system. Additionally, platelets contain granules containing von Willebrand Factor (vWF), platelet-activating factor, and other platelet activating materials(7, 8) .

Activation of platelets is initiated by a rupture in the vessel endothelial lining, exposing von Willebrand Factor (vWF) and extracellular matrix proteins, such as collagen, to the blood. This contact between surface receptors on the platelet with these proteins causes the conformational changes in platelets by extending their pseudopodia

contained within the canalicular system (8). Translocation of the pseudopodia exposes the anionic phospholipid layer on their outer surface for attachment of other platelets, vWF, and other proteins(8-10) .

The mechanism behind the translocation is caused by a platelet membrane receptor, GPIa, which induces the platelet conformational change (see Figure 1). This change exposes a second platelet membrane receptor GPIb and in the presence of vWF, induces greater conformational change. This greater change exposes the GPIIb/GPIII receptor proteins, allowing for binding of more collagen and vWF(8).

Once platelets are activated, these platelets begin to adhere to one another, in a process called platelet adhesion. Just as the activation cause the extension of the pseudopodia and adhesion, it causes the granules to be released from the canalicular system as well. By releasing the granules, this creates more soluble vWF to activate more platelets (8) .



Now with activated platelets, this self-sealing system employs the combination of the

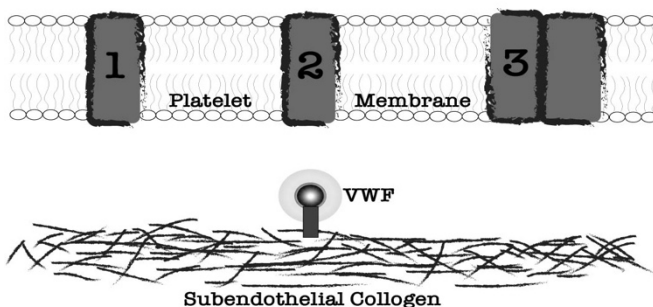


**Figure 1.** Platelet Adhesion Steps. GpIa binds the exposed subendothelial collagen (Step 1) and allows GpIb to bind vWF (Step 2). This binding with vWF exposes the (Step 3) GpIIb-GpIIIa complex. This image was adapted from: Lieberman M, Marks AD. Marks' basic medical biochemistry

tissue factor pathway and the contact activation pathway; termed extrinsic and intrinsic pathways, respectively. These pathways are a series of sequential reactions, in which the inactive enzyme precursors (zymogens) of a serine protease activates to become an activated serine protease. The

coagulation cascade zymogens are called Factors and identified by Roman numerals (see Table 1 for a list). Once the Factor has been activated its name indicates so by following the name with the letter "a"; i.e. Factor IX (FIX) activated is Factor IXa (FIXa). That serine protease plants on the phospholipid surface provided by the platelet, thus catalyzing the next reaction in the cascade by cleaving the downstream substrate. The intrinsic and extrinsic cascades work in tandem having the goal of activating Factor X (FX), prothrombin (FII), and cleaving fibrinogen (FI) (11-15) .

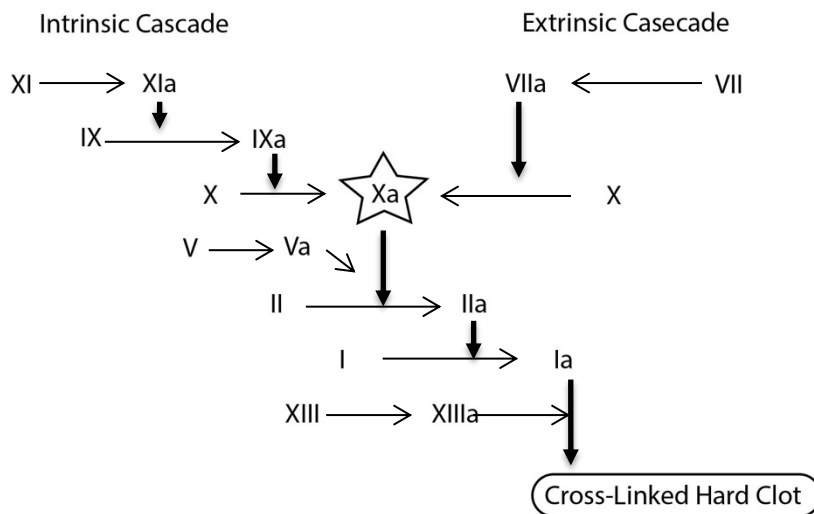
**Table 1 Blood Coagulation Proteins.**

Blood Coagulation Proteins with Common Name, Descriptive Name, and Function. An activated form has an "a" added to the common name. An \* indicated the proteins that are Vitamin K dependent.

<i>Common Name</i>	<i>Alternative Descriptive Name</i>	<i>Function/Active Form</i>
FI	Fibrinogen	Fibrin
FII*	Prothrombin	Serine protease
FIII	Tissue Factor(TF)	Receptor, Cofactor, and Initiator
FIV	Ca <sup>2+</sup>	Cofactor
FV	Proaccelerin, labile factor	Cofactor
FVII*	Proconvertin	Serine protease
FVIII	Antihemophilia factor A	Cofactor for FIX activation
FIX*	Antihemophilia factor B, Christmas factor	Serine protease
FX*	Stuart-Prower factor	Serine protease
FXI	Plasma thromboplastin antecedent	Serine protease
FXII	Hageman Factor	Serine Protease
FXIII	Fibrin-stabilizing factor	Ca <sup>2+</sup> -dependent transglutaminase
Thrombomodulin		Thrombin Cofactor in Protein C Activation, Endothelial Cell Receptor
Protein C*		Serine Protease, Activated by Thrombomodulin-bound thrombin
Protein S*		Cofactor for activated Protein C
Antithrombin III	ATIII	Protease Inhibitor

The Extrinsic pathway, as seen in figure 2, is composed of Tissue Factor (TF) and Factor VII (FVII) to activate FX (16). TF is expressed on subendothelial tissues and fibroblast cells outside of the vasculature. This is vital for pinpoint identification of a vascular break and formation of the TF-FVIIa complex (3, 17, 18). The TF-FVIIa complex then activates FX and FIX (19, 20).

The Intrinsic pathway is composed Coagulation Factors IX, VIII, and XI (see Figure 2). Again, the goal is to activate Factor X and ultimately generate a thrombin burst. The pathway starts with the activation of FXII that converts FXI to FXIa. FXIa then cleaves FIX, activating to create FIXa. Then FIXa interacts with FVIIIa to form the tenase complex, whose role is to activate FX into FXa (12).



Extrinsic and intrinsic pathway activation results in the activation of the common pathway for a favorable thrombin generation state (see Figure 2). The central objective of the common pathway is to activate FX,

**Figure 2.** Blood Coagulation Cascade showing the overall goal of activation of FX to Xa to for the prothrombin complex to form a hard fibrin clot. Not shown are the necessary cofactors that are required for full procoagulant activity. Adapted from: Lieberman M, Marks AD. Marks' basic medical biochemistry: A clinical approach. 4th ed. Lippincott Williams & Wilkins; 2012.

thrombin, and fibrin, inducing clotting. This central objective is best achieved when coagulation is viewed as the Cell-Based Model for Coagulation (CBMC) (21). The CBMC model accounts for the fact that both pathways are necessary to form a fibrin clot and that if one is deficient this leads to clinical issues such as hemophilia or spontaneous clot formation. CBMC is a four-step process for coagulation, composed of Initiation, Amplification, Propagation, and Termination (21).

Initiation occurs when trauma leads to the exposure of TF, extracellular collagen, and von Willebrand Factor (vWF) (13, 17, 22). These indicators allow for injury site detection with pinpoint precision and initiate a response. Platelets, activated by vWF and extracellular collagen, extend their pseudopodia. The activation of platelets and exposure of the TF bearing tissue to circulating blood is important for providing an anionic phospholipid layer for the coagulation factors to sit on (12, 23).

Simultaneous to the platelet activation is the formation of a complex between Coagulation Factor VII (FVII) and Tissue Factor (TF) (23). FVII activation is brought about by auto-activation or activation by trace amounts of FXa (24). Formation of this complex activates a small amount of FIX and FX via proteolytic cleavage, producing FIXa and FXa (10, 25, 26). This small amount of FXa will activate a small amount of thrombin needed to allow for progression to amplification.

Amplification started with the initiation step providing the necessary materials of activated FIX, FX, and importantly thrombin. The small amount of thrombin generated during initiation activates FV, FVIII, and FXI. FXIa is a potent activator of FIX, and FVa is an important cofactor for FXa (27, 28). FVIIIa is an important cofactor for FIXa and

thrombin spurs its release from vWF to bind with FIXa. With these cofactor and factors activated, it amplifies the quantity of pro-coagulation complexes to proceed into the propagation phase (11, 29).

Propagation is a fully primed intrinsic/extrinsic response to generate fibrin. On the platelet surface the tenase (Xase) complex of FVIIIa and FIXa activates FX to FXa. FXa then forms the prothrombinase assembly with FVa to convert prothrombin to thrombin (8). This functional prothrombinase assembly generates the thrombin burst. This thrombin burst catalyzes the cleavage of fibrinogen into fibrin thus forming the clot at the area of injury. The insoluble fibrin monomers aggregate together to form a soft clot. Activation of FXIII to FXIIIa (Transglutaminase) then crosslinks the fibrin clots. This cross-linking forms a rigid network trapping the platelets and erythrocytes inside, forming the hard clot.

Termination, the fourth step of CBMC, is continually ongoing as it employs multiple routes to keep the other three coagulation steps in check. This process ensures healthy vasculature does not form random clots and dissolves the clots that have formed. Formation of spontaneous clots could lead to clinical issues such as thrombus and ultimately result in an embolism (21).

To accomplish this never-ending task, termination employs the Protein C/Protein S/Thrombomodulin System (21). Protein C is an anticoagulant zymogen, when bound to its cofactor thrombomodulin (TM) (5, 30-33). TM inhibits the clotting abilities of thrombin and activates Protein C. Activated Protein C binds with cofactor Protein S to form the

Protein C-Protein S complex that can terminate thrombin generation on platelets by destroying FVa and FVIIIa (34, 35).

Fibrinolysis, the process of breaking down a formed clot occurs as part of normal wound healing. The primary enzyme that breaks down the fibrin clot is plasmin. The inactive pro-enzyme, plasminogen, flows throughout the blood and activates on contact with the clot surface to form plasmin. Activation occurs by activator proteins called tissue plasminogen activator (tPA) and single chain urokinase (scu-PA). Plasmin begins to break down the fibrin resulting in full dissolution of the clot once the wound has fully healed.

### **1.3 Serine Proteases**

Hemostatic regulation occurs through the employment of coagulation factors known as serine proteases. Serine protease production occurs in the liver's hepatocytes and then they circulate as zymogens in the blood. Proteolytic cleavage turns these inactive enzyme precursors into active serine proteases. Minute differences allow them to operate with the high degree of specificity to provide precision with regulation.

All serine proteases share a great deal of similarity in gene sequence (29, 36, 37). Sharing a high degree of DNA and amino acid similarity, protein folding delivers similar structure patterns throughout the serine proteases. As demonstrated in the general clotting factor structure shown in Figure 3. The clotting proteases are composed of a catalytic head, two Epidermal Growth Factor (EGF)-like domains, and a Gla domain (29, 38, 39). This can be best imagined if thought about as a Venus Flytrap.

The catalytic head resembles the digestive enzyme trypsin and forms the “fly catching portion” of the flytrap. The catalytic head contains the protease domain to hydrolyze peptide bonds by utilizing a “catalytic triad” of Serine, Histidine, and Asparagine (40-43). This “catalytic triad” is responsible for the activation of the next sequential protease.

Holding up the catalytic head like a stem, are the two EGF-like domains. The primary role of EGF-like domains is to hold the catalytic head off the phospholipid surface and into the space above (41, 42, 44). This area also contains some binding sites for regulators and co-factors of the enzyme. A flexible linker attached to the two EGF-like domains holds the catalytic head (41, 42).



**Figure 3** Structure of coagulation factor. The EGF1 and EGF2 domains are the “stem” portion holding up the catalytic head. The “root” of the structure is the Gla domain, that anchors the coagulation factor to the phospholipid surface.

The Gla domain refers to the conserved feature of amino-terminal carboxylated glutamic acid residues that serve to anchor the entire structure (41). These modified residues serve to anchor the entire structure via calcium bridging to the phospholipid surface (38, 39, 44). The interaction of the Gla domain is possible by the Vitamin K dependent,  $\gamma$ -carboxylase modification to the glutamate residues during synthesis in hepatocytes of the liver (24).

The  $\gamma$ -carboxylation occurs via a quinone reductase that reduces Vitamin K to  $KH_2$ . Carboxylase enzyme cofactor Vitamin  $KH_2$  adds the carboxyl group to the Gla domain. Calcium with a positive charge chelates via electrostatic interaction the negative charged Gla domain and the anionic head group of phospholipids (25, 41).

Coagulation factors employ cofactors to assist in the protease activity. These cofactors are comprised of factor specific cofactors in addition to the universal cofactors. This relationship allows for pivotal coagulation cascade reactions to occur through improved posturing of the factor/substrate orientation.

Universal Cofactors that are required by all serine proteases in the coagulation cascade are calcium and an anionic phospholipid membrane. Radcliffe *et al.* found that adding phospholipids and  $CaCl_2$  caused an 11-fold increase in activation of FVII (22). Calcium serving as a cofactor with a positive charge chelates via electrostatic interaction the negative charged Gla domain and the anionic head group of phospholipids (25, 41). The interaction between the Gla domain and EGF-like domains is also highly dependent upon calcium for orientation on the membrane in the vertical position of the serine proteases, as described by Bode *et al.* 1997 (32). Krishnaswamy *et al.* also



demonstrated evidence that substrate-membrane interaction considerably enhances activation of FX by the extrinsic Xase complex (14, 45, 46). Without proper vertical orientation and attachment to the phospholipid membrane the serine proteases exhibit very reduced activity (45).

Though all serine proteases share a great deal of similarity in DNA and amino acid sequence they are highly specific for activation, cofactor, and substrate (29, 36, 37). Important cofactor/factor relationships that greatly increase protease activity are: FVIIIa to TF, FVIIIa to FIXa, and FVa to FXa. These specific relationships are what give way for an optimal  $K_m$  and  $K_{cat}$ .

As previously mentioned, the key role of FXa is to activate FII. FX activates prothrombin via two methods and speeds: FXa alone slowly or at exponentially greater rate with the cofactors in the prothrombinase complex. The prothrombinase complex forms when there is vascular injury, and the platelet provides a phospholipid surface for FXa, with cofactor FVa, acting on the substrate, Prothrombin. Specifically, FXa performs activation of FII via proteolytic cleavage of two peptide bonds on the heavy chain, turning FII into FIIa (46).

To best understand the role of serine proteases and their respective cofactors it is important to look at Protein C, a serine protease whose function is to oppose coagulation. Activated Protein C (APC) is crucial to the regulation of the clotting cascade by acting on procoagulant serine proteases. Protein C shares similar structure and generation to the Vitamin K dependent, pro-coagulant serine proteases synthesized in the liver (30). APC in complex with cofactor Activated Protein S (APS), forms the

APC/APS complex that is responsible for degradation of FVa and FVIIIa. Protein C is activated by thrombin, and this activation is enhanced when thrombin is attached to thrombomodulin. Thrombomodulin is a cofactor for thrombin found on the surface of endothelial cells (34, 35). Walker *et al.* found that Protein C has a high degree of specification and once activated cleaves both chains of the activated clotting enzymes, FVa and FVIIIa (14, 30). Just as with FXa alone can activate a small amount of prothrombin, it was identified that Protein C can inactivate FVa and FVIIIa independently, but the  $K_m$  is substantially decreased by the cofactors (30). Interestingly it was discovered that the complex is not able to inactivate FVIIIa when, FVIIIa is coupled with cofactor vWF (35).

FVIIa bound to TF in association with calcium on phospholipid surface forms the extrinsic tenase complex and is the preliminary activator of FX (17, 22, 47). TF presiding as the cofactor for FVIIa embraces the protease in optimal vertical orientation off the membrane surface (48). McCallum *et al.* demonstrated the ability of the cofactor to be so necessary for orientation it allows for prime positioning even if the Gla domain of FVIIa becomes detached (18, 26, 49).

Kovalenki *et al.* investigated the activation of FX to FXa by the extrinsic tenase complex and found that the size of the vesicle affected the rate of the reaction (50, 51). This is important because it draws attention to the topographical and geometrical limits of the factors while sitting vertically on the phospholipid membrane

## 1.4 Factor IX

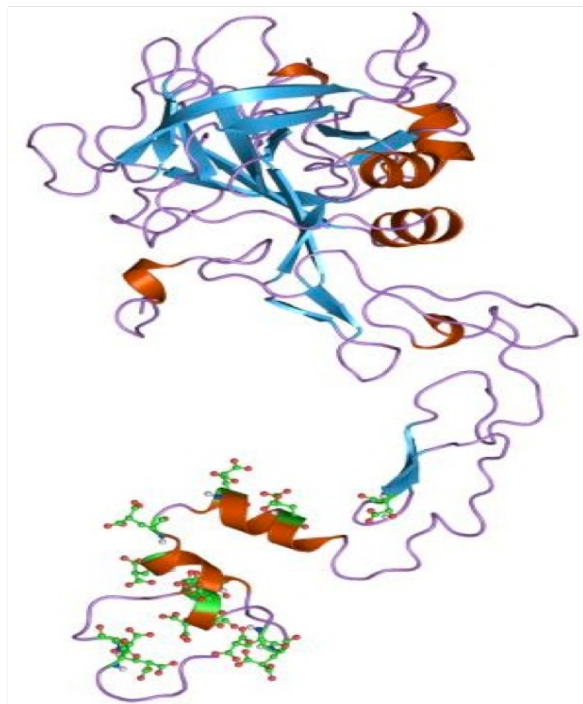


**Figure 4** Structure of Factor IX in Ribbon View with protein structure.

Photo by Jawahar Swaminathan and MSD staff at the European Bioinformatics Institute / Public domain

identified the disease as being a unique form of hemophilia. This mutation resulted in a cysteine changed into a serine on the X chromosome within what is now identified as the FIX gene (52-55).

The general structure of FIX shares a similar homology with the other serine proteases (see figure 4). More specifically FIX is composed of two chains equaling 415 amino acids, a C-terminal heavy and N-terminal light chain (52). The C-terminal Heavy chain of 235 amino acids forms from residues 181 to 415 (44). The N-terminal light

Factor IX (FIX) shares similar homology with other vitamin K dependent clotting factors produced in the liver. It is an essential clotting factor and a deficiency in FIX can lead to clinical issues such as hemophilia B, also known as Christmas Disease (52, 53). Analyzing the DNA sequence data of the proband patient who had a bleeding disorder

chain consists of 145 amino acids (39). Together light and heavy chains are linked with a disulfide bond at Cys-132 and Cys-189 (40-43).

This heavy chain contains the FIX catalytic head region as previously described in the general description of serine proteases. The importance of the FIX catalytic head is that it specifically contains the "Catalytic Triad" composed of Histidine-236, Serine-365, and Asparagine-269 (40-43). This catalytic triad is responsible for the activation of FX.

The N-terminal light chain includes the Gla domain and two EGF-like domains (39). The Gla domain of FIX is composed of the amino acid residues 1-38, which anchors the enzyme with the calcium bridge to the phospholipid membrane of the platelet or other phospholipid surface (39, 44). EGF-like domains are residues 47 to 84 and 85 to 127 (42). There is also a hydrophobic helix at residues 39 to 46, which acts as a support for the EGF-like domains (41). Both EGF-like domains are stacked and joined with a convex hydrophobic loop of EGF1 and a concave hydrophobic socket of EGF2 (41). A flexible linker with residues 128 to 145 holds the catalytic head (41, 42).

Activation of FIX occurs by the intrinsic and extrinsic pathways. FXIa is the activator in the intrinsic pathway model and FVIIa in the extrinsic pathway. FIX activation is in two cleavage events performed by FVIIa/TF or FXIa (56). The first cleavage generates FIX $\alpha$  with a single cleavage removing Arg-180 to Val-181, followed by a second cleavage removing Ala-146 to Arg-180 to generate FIX $\alpha\beta$  (42, 57).

Fully activated FIX $\alpha\beta$  forms the Xase complex, with specific cofactor FVIIIa and universal cofactors. The role of FIX catalytic head is activation of FX by hydrolysis of peptide bonds at Arg-194 to Ile-195 (40-43). This complex has been demonstrated to

have  $10^9$ -fold increase in the procoagulant activity compared to active, non-complexed FIXa, as reviewed by Neuenschwander *et al.* (56, 58).

The anticipated height of FIXa is a distance between 50 to 100 Å above the membrane. A review and understanding of the FIXa structural dependency on cofactors is fundamental. X-ray crystal structures have demonstrated the ability of cofactors and ions to change the conformation of factors in the clotting cascade. Length changes of the serine protease, specifically FIX have been demonstrated with cofactors. Bode *et al.* and McCallum *et al.* determined how the interaction between the EGF1 domain and Gla domain is highly dependent upon calcium (41, 59). When there is a lack of calcium the protease is no longer able to chelate to the phospholipid surface. Also, through small angle x-ray and NMR studies, a change in orientation based on calcium has been detected (41, 44). The EGF-like domains' binding sites for cofactor FVIIIa act upon the final structure of Xase complex. When bound, they promote activation of FIX by holding in the vertical orientation (41). While all of these studies point to the orientation of the complex, none are capable of addressing the specific optimal distance and orientation of the catalytic head with regard to stretch and flexibility of the factor (60).

### **1.5 Anti-Coagulation and Inhibitor Structure**

Anticoagulants are chemicals used in the prevention of blood clotting by acting on clotting factors within the Coagulation Cascade. Anticoagulants have a long history of uses throughout evolution by animals such as mosquitos to obtain blood from the host animal (61). Currently, anticoagulants are used as therapies in patients, for example with atrial fibrillation to prolong an individual's survival. Most of the current anticoagulant therapies used in medical practice involve coumarins and heparins (62).

Looking at the mechanism by which coumarins work it is important to look specifically at the drug Warfarin. Warfarin first used by man as a rat poison was later approved for use as an anticoagulant by acting as a Vitamin K analog (63). Vitamin K activity is impeded by Warfarin interacting with Vitamin K epoxide reductase. Without enough active Vitamin K to carboxylate the Gla residues on Vitamin K dependent serine proteases they are no longer able to chelate the phospholipid surface (21, 44). This is a common way to prevent blood coagulation but has negatives to its uses such as a drug loading time, taking around 72 hours before effects are seen in a patient.

The polymer, heparin is another common anticoagulant used by medical professionals in things such as blood filtration procedures and surgeries. Heparin is naturally produced in the body by basophils and mast cells and can be extracted for pharmaceutical uses from mammals such as cattle and pork. Heparin works by binding and increasing activity of Antithrombin III (AT) (15, 32, 61, 64-66).

Antithrombin (AT) belongs to a class of inhibitors known as serine protease inhibitors or serpins. Serpins contain a serine residue in their catalytic triad to help regulate the proteolytic clotting cascade. A principal class of serpins is Kunitz Protease Inhibitors, which includes AT. AT is a small glycoprotein produced in the liver, which binds to the serine residue in the active catalytic triad of thrombin, leaving it inactive. Other common serpins of FXa and FIXa are Basic Pancreatic Trypsin Inhibitor (BPTI) and Protease Nexin-2, respectively, via their Kunitz Protease Inhibitor domains (58, 67). To tie this together heparin has also been shown to increase the rate of AT and FIXa inhibition in the presence of  $\text{Ca}^{2+}$  (58).

## **2 Research Design**

As discussed, blood coagulation requires the use of enzymes orchestrated in a series of highly specific events. For these events to occur at a tremendous exponential rate, the enzymes require their respective cofactors and a phospholipid membrane. It has also been determined that the topographical characteristics of the activation complex on the phospholipid membrane are also essential. Fluorescence studies have delved into the distance of closest approach to the membrane of the active site for several of the coagulation serine proteases (42-44, 49, 59, 60, 68, 69). In several instances, it was documented that the non-enzymatic cofactor binding altered the distance. With distance above the membrane correlated to the overall length of the serine protease as determined by x-ray crystal structures, it is reasoned that proteases orient vertically on the membrane with little to no bending (Figure 5). This reasoning has not been proven using fluorescence resonance energy transfer (FRET)-based studies as these are only capable of showing the distance of closest approach. FRET cannot determine the optimal height/distance needed for maximum coagulation activity. Also, lacking in the gap of knowledge is the potential for elasticity and their ability to stretch off the membrane, proving to be a significant gap in knowledge. **The goal of this study to gain insight into the optimal reactive height of coagulation factor IXa above the phospholipid surface by the generation of a lipid Anchored Molecular Ruler with attached Inhibitor (AMRI).**

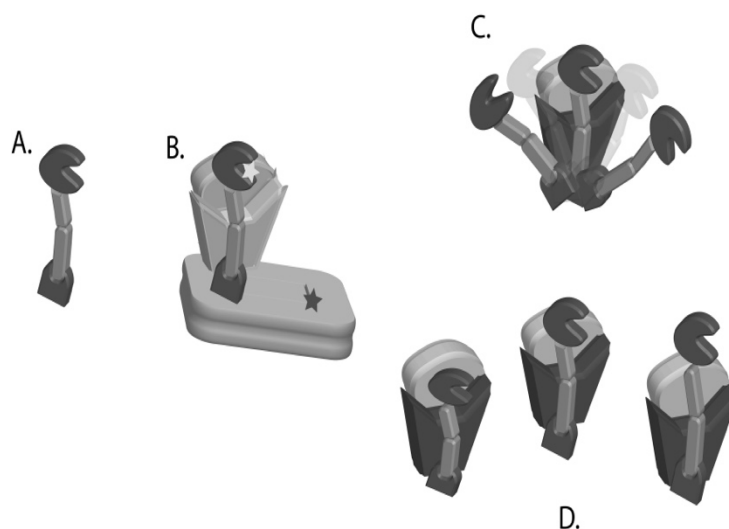


**Figure 5** Demonstration of knowledge lacking in the optimal reactive height of FIXa. This looks at Crystal Structure Data (A) and FRET (B). The Crystal structure gives us the height at a moment frozen in time. FRET data gives the distant of closest approach. Lacking is the information on the wobble (C) and the stretch (D) to understand how the Factor moves in a fluid environment for optimal reactivity.

The enzymatic characterization of coagulation factors has been frequently studied through use of small peptide inhibitors such as serpins, as they sit directly in the catalytic site of the enzyme (38, 70-73). Hence, we are using it in the AMRI. To generate AMRI, a protein anchoring sequence of Leucine, Alanine,

Glycine, and Cysteine (LAGC) is used to fixate the entire structure to a lipid surface. To direct the lipid-bound protein for anchoring, LAGC will be coupled with a leader sequence for shuffling into periplasmic space, originally from the Apyrase gene of *Shigella*, for protein collection. A height adjustable linker area is then required between the anchor and inhibitor regions of AMRI to ensure the proper height of inhibitor. Employing the linker sequence EAAAK, with a rigid slantwise fixed height of 7.5 Å per sequence, will allow for the creation of a specific height for the engineered protein (74). Based on the Crystal structure data the hypothesized reactive height is a distance between 50 to 100Å above the membrane (6, 42, 43, 69). Completing the protein's linker



region will be a flexible linker at the end of a rigid set to ensure the inhibitor properly fits in FIXa active site. Finalizing the AMRI complex will be a PN2-KPI inhibitor, which has previously been demonstrated to inactivate FIXa.

### **2.1 *Protease Nexin2 - Kunitz Protease Inhibitor (PN2-KPI)***

Anchored Kunitz-based inhibitors bound to lipid membranes have been successfully utilized for analysis of serine protease activity using Surface Plasmon Resonance (SPR). SPR allows for measurement in a real-time binding of two molecule companions without the need of labels by detecting the changes in refractive index (GE Healthcare, Technology Note 23: Label-free interaction analysis in real-time using surface plasmon resonance. (2007) BR-9004-63 28-9214-39 AA.). The researchers generated a phosphatidylcholine (PC) lipid monolayer containing nickel chelating head groups and successfully attached 6-histidine-tagged bovine pancreatic trypsin inhibitor (BPTI). Over the attached BPTI lipid layer, soluble proteases flowed over and were bound, establishing proof that a bound Kunitz inhibitor is capable of remaining functional after attachment. However, these studies found that binding rates were drastically lower than in other studies using solution-phase testing (56, 58). One explanation of this is the desired orientation of proteases on the membrane and the close position of the inhibitor on the membrane. This negative steric interaction is the reasoning for wanting the Kunitz inhibitor attached at a set distance above the membrane and allowing more favorable binding to the protease domain.

The Kunitz Protease Inhibitor domain of Protease Nexin 2 (PN2) was employed to bind to the active site of FIXa (56, 71). The precursor form of this protein, PN2-Amyloid  $\beta$  Protein Precursor (A $\beta$ PP) was found to have a role in the regulation of specific

proteases in extracellular environments; specifically, with plaque deposits of those affected with Alzheimer's disease and Down syndrome (72). Schmaier *et al.* found that PN2-A $\beta$ PP was 71-fold more effective in ability to inhibit FIXa than antithrombin III (70, 71). Neuenschwander *et al.* experimentally determined that using just the inhibitor domain of PN2 (PN2-KPI) displayed an increased affinity for FIXa (58). PN2-KPI is a more ideal inhibitor for height determination of the FIXa active site.

## **2.2 LAGC anchor with Apyrase leader sequence**

Hydrophobic anchoring of a protein to a lipid membrane is not a novel idea, but an evolved mechanism. In unicellular organisms many membrane proteins utilize the Lipobox motif to anchor to the phospholipid. Roughly 75% of all lipobox sequences consist of the amino acid sequence, LAGC. The cleavage between the Glycine and Cysteine results in the formation of an N-terminal Cys. The SH group on the new N-terminal Cys is acted on by diacylglycerol transferase, creating the diacylglyceryl moiety. This moiety with Cys incorporated serves as the anchor to the phospholipid surface so that the attached protein does not diffuse away (75).

Bhargava *et al.* identified a 23 amino acid leader sequence for virulent apyrase gene that is responsible for translocation of the protein from the cytosol to the periplasmic space in Gram-negative bacteria. Identification was possible via cloning and expression of *Shigella flexneri 2a* apyrase gene in an *E. coli* plasmid (76). Apyrase was directed to exit the cytosol and travel to the periplasmic space through translocase. The leader sequence on the N-terminal end is recognized and transported to the periplasmic space. The clone was then sequenced against the wildtype for confirmation of the apyrase gene.

Kamalallannan *et al.* demonstrated an engineering process for converting a non-lipoprotein into an anchored lipoprotein (75). Using the *Shigella* apyrase leader sequence for transport, anchoring with LAGC sequence combined with normal protein sequence generated a viable lipid bound protein. With the Cys serving as the anchor on the N-terminus end, it allowed for regular protein expression on the C-terminal end.

### **2.3 Linkers= (EAAAK)<sub>11</sub> (GGGGS)**

Linker construct has become an essential tool in the development of protein fusion. The ability to link proteins and not interfere with their reactivity is vital and achieved by taking into consideration flexibility and hydrophilicity (77, 78). The sequence EAAAK, whose parent strand, initially described by Marqusee and Baldwin in 1987, is referred to as a rigid linker, forming alpha helices (78). This helix is stabilized by Glutamic acid and Lysine salt bridges and internal Hydrogen bonds (74, 77-79). Arai *et al.* determined that it was possible to control the distance between two proteins by manipulating the repetition of the EAAAK motif (77, 80). Amet *et al.* described the use of EAAAK linker sequence by varying the number of sequence repeats to optimize reactivity of an expressed protein (81).

As the number of EAAAK motif repeats increases, so does the strength and tightness of the alpha helix structure (80). Through FRET studies and high-resolution models, it also determined that the linkers connect diagonally and not longitudinally creating a vertical increase of 7.5 Å and not the interdomain distance of 10 Å, with (EAAAK)<sub>5</sub> having a distance of 43.86 Å (74, 77, 80). It was concluded that the rigid linkers provided a lesser degree of distance fluctuation between the N and C terminus.

Li *et al.* also confirmed through molecular dynamic simulation that EAAAK in helical form is in the lowest energy state, indicating conformational stability (74).

The GGGGS sequence is a well-known flexible linker with many applications in

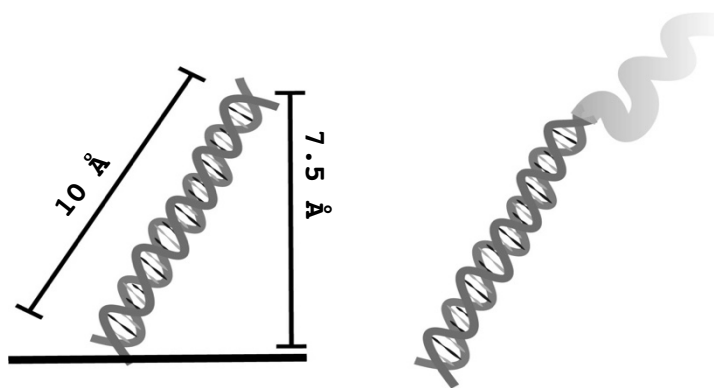


**Figure 6** Structure formations of EAAAK and GGGGS. This demonstrates how the proposed protein structure will be rigidly lifted from the phospholipid membrane, while GGGGS provides the flexible conduit for proper insertion of the inhibitor

protein engineering. This flexible nature allows for the mobility of the inhibitor and the tethered EAAAK rigid sequence. In the Li *et al.* 2015 study on molecular dynamics, it was found to have no energy change in the 29ns simulation and produced total energy fluctuation the entire time (74). This is indicative of a protein with no conformational stability. The flexible linker also produced an increase in variable distances in the FRET analysis conducted (74, 80). Incorporation of the flexible linker at the end of the rigid linker sequence supplies a lack of conformation, making it ideal to serve as the "intermediary" between the rigid linker and inhibitor. This lack of conformity will provide the inhibitor with freedom of movement to fit within the catalytic head of FIX.

## **4 Specific Aims**

The focus of this study is to generate a lipid **A**nchored **M**olecular **R**uler with attached **I**nhibitor (AMRI) at a fixed height to quantify the optimum reactive height for FIXa. The hypothesized reactive height is a distance between 50 to 100Å above the membrane.

Specific Aim 1: Creation of an AMRI in an expression vector.

Specific Aim 2: Purification of AMRI in an expression vector.

Specific Aim 3: Sequencing of AMRI in an expression vector.

## **5 Methods**

### **5.1 SnapGene**

SnapGene® software (from GSL Biotech; available at [snappgene.com](http://snappgene.com)) was used for vector mapping and design. The PCR primers and oligonucleotides were designed with the program including the LAGC anchor region to attach to a phospholipid membrane; an EAAAK (EA<sub>3</sub>K) rigid linker serving as a molecular ruler; a PN2-KPI region serving as the FIXa inhibitor; the PCR primers needed to correct the orientation of the current p-LAGC-EAK10 plasmid.

### **5.2 Vector Preparation**

#### **5.2.1 Description**

pET11d plasmid was used for the cloning backbone. The p-LAGC-EAK10 plasmid was a gift from a previous GA-PCOM thesis student. This plasmid contained the *Shigella* apyrase leader sequence, anchor sequence LAGC, and the molecular ruler sequence of EAAAK repeated 10 times inserted between the *Nco*I and *Hind*III restriction sites.

### **5.2.3 Growth**

Streak plates of DH5 $\alpha$  *Escherichia coli* (*E. coli*) were made with LB agar (10 g/L tryptone, 5 g/L yeast extract, 10 g/L NaCl, 15 g/L Difco Granulated agar, pH 7.0) containing ampicillin with a concentration of 50  $\mu$ g per ml (82) . The plate was placed in 37°C incubator overnight and removed after growth and placed in 4°C for storage. Individual isolated colonies were chosen and inoculated into 5 ml culture tubes, containing LB media. Ampicillin ensures the selection of only *E. coli* containing any vector with the gene conferring Ampicillin resistance; inhibiting growth of *E. coli* lacking ampicillin resistance. The culture tube was then placed in a 37°C incubator at 250 rpm overnight. This growth was to ensure a good cloudy density of bacterial growth. 1 mL of the initial 5 mL culture was used to inoculate 250 mL and 500 mL LB media cultures.

### **5.2.4 Transfection**

Competent DH5 $\alpha$  *E.coli* cells were used for transfections and were a gift from Dr. Frank Jenney. The DH5 $\alpha$  cells were taken from the -80°C freezer and placed to thaw on ice. The cells were then stirred with the tip of a pipet, before pipetting 70 $\mu$ l into a pre-chilled 1.5 ml tube. There as one tube per each individual reaction. 10 ng of plasmid DNA was placed into the 70  $\mu$ l of competent cells and stirred with a pipet tip. This mixture was then placed on ice to incubate for 30 minutes, followed by 30 seconds of incubation at 42°C to heat shock the cells. The tubes were immediately transferred and chilled on ice for 2 minutes. Next, 300  $\mu$ l SOC (20 g/L tryptone, 5 g/L Yeast extract, 0.5 g/L NaCl, 10 ml/L 250 mM KCl, 5 ml/L 2 M MgCl<sub>2</sub>, 20 ml/L 1M glucose, pH=7.0)

prewarmed to 37°C was added to the cell mixture and allowed to shake for 1 hour at 100 RPM. The cells were then plated 100µl and 200µl on LB plates, both with and without the 50 µg/mL ampicillin selection agent. In these experiments, different molar ratios of the digested vector and insert were used to obtain optimum transfection efficiency. Experimental molar ratios of 1:3 and 1:6 vector to insert were used. Controls included vector plus ligase only, and DH5α cells only. Once plated the plates were allowed to dry before placing inverted at 37°C overnight. Isolated colonies on the successful plates were then inoculated into an LB broth with ampicillin as described above.



### **5.2.5 DNA Miniprep**

DNA Miniprep was performed to screen for the intended clone at various stages of the cloning process. Quantum Prep® Plasmid Miniprep Kit (Bio-Rad Laboratories Inc., Hercules, California, Catalog #732-6100) was used in all Miniprep procedures. During this process, centrifugation was performed at the maximum speed of 13,300 x *g* on a tabletop centrifuge. Using 1 to 2 ml of the growth culture the protocol was followed depending on the desired final concentration of pure plasmid. The culture was placed in a microcentrifuge tube to pellet the cells and ran for 30 seconds. With the cells pelleted the supernatant was removed by pipetting. Then another quick spin on a small desktop centrifuge was performed just to ensure removal of supernatant. The pellet was resuspended using 200 µl of the Cell Resuspension Solution provided by vortexing and pipetting up and down. Next 250 µl of the Cell Lysis Solution were added and mixed by gently inverting the capped tube about ten times. The Cell Lysis Solution was followed by the addition of 250 µl Neutralization Solution then inverted 10 times for complete mixture. A precipitate formed and was then placed back in the centrifuge for 5 minutes to collect the cell debris. The plasmid DNA, located in the clear lysate, was transferred to a spin filter, and combined with 200 µl mixed Quantum Prep Matrix, with the filter placed in a 2 ml centrifuge tube. The tube with the filter was centrifuged for 39 seconds. The spin filter was removed, and filtrate discarded, then put back in the centrifuge tube and washed twice with 500 µl of Wash Buffer. The first wash was centrifuged for 39 seconds and the second was for 2 minutes. An additional spin was performed if a slight smell of ethanol persisted. The filter was then placed in a 1.5 ml microcentrifuge tube

and eluted for 1 minute with 100  $\mu$ l of prewarmed 70°C nuclease-free water. The purified DNA was then either stored at -20°C or used immediately.

### **5.2.6 DNA Midiprep**

Quantum Prep™ Plasmid Midiprep Kit (Bio-Rad Laboratories Inc., Hercules, California, Catalog Number 732-6120) was used for collection of larger pure plasmid DNA amounts. All centrifugation was in a swing bucket table-top centrifuge using 250 ml Oak Ridge tubes. 250 ml growth media was centrifuged at 5,000  $\times g$  for 10 minutes to pellet the cells. The tubes were then drained of supernatant and inverted on a paper towel to ensure removal of media. The pellet was resuspended with 6 ml Cell Resuspension Solution and mixed by vortexing until all cells were back in solution. Next, 6 ml of prewarmed 37° Cell Lysis Solution were added and mixed by rolling on the benchtop. This mixture was allowed to sit for 3 minutes at room temperature before adding 10 ml Neutralization Solution and mixed by inverting 5 times. After 3 minutes a white flocculant formed. This solution was then placed in a PureYield™ Clearing Column and a new 50ml disposable Falcon plastic tube, then allowed to sit for an additional 2 minutes at room temperature before centrifuging at 2,500  $\times g$  for 10 minutes. Then filtered lysate was transferred into a PureYield™ Binding Column and new 50ml disposable Falcon plastic tube to which 5.0 ml of Endotoxin Removal Wash Solution were added. This was centrifuged at 1,500  $\times g$  for 3 minutes, and the flow through was discarded. Following the Endotoxin Wash were two washes of 20ml of Column Wash Solution, discarding the flow through each time. At the completion of the second wash, the column tip was tapped dry on a paper towel and placed in a new

Falcon tube and spun for 15 minutes at  $1,500 \times g$ . The column was then allowed to sit for 5 minutes or until no smell of ethanol remained. Next, the column was placed in a new Falcon tube, and 600  $\mu\text{L}$  of prewarmed  $70^\circ\text{C}$  nuclease-free water was allowed to sit on the column membrane to rehydrate. After 2 minutes the tube was centrifuged for 5 minutes at  $1,500 \times g$ . The filtrate was collected and placed in a 1.5 centrifuge tube.

### **5.3 DNA Analysis**

#### **5.3.1 Thermo Nanodrop Spectrophotometer**

The ThermoFisher Scientific Nanodrop Spectrophotometer, now referred to as NanoSpec, was started using the setting for double-stranded DNA and was calibrated using only 2  $\mu\text{L}$  of nuclease-free water. Then 2  $\mu\text{L}$  of DNA sample was added to the NanoSpec to determine concentration ( $\text{ng}/\mu\text{L}$ ). The NanoSpec made measurements by wavelength absorbance at 260 nm for Nucleic Acids and 280 nm for proteins. This  $A_{260}/A_{280}$  ratio reading was calculated to determine DNA purity; a ratio of close to 2.0 is considered pure for DNA, however anything above a 1.8 was considered acceptable for use.

#### **5.3.2 Agarose Gel Electrophoresis**

A 1% agarose gel (10 mg/mL of Nuclease-free agar in 1X TAE Buffer (Tris-acetate-EDTA, pH 8.3)) was separated using 0.1  $\mu\text{L}/\text{mL}$  GelRed™ Nucleic Acid Gel Stain

(Phenix Research Products, Candler, North Carolina) in 1X TAE running buffer. For tracking the progression of DNA in the agarose, 5  $\mu$ L Quick-Load 2-Log DNA Ladder (New England BioLabs, Ipswich, Massachusetts, Catalog # N0550S) was employed for size analysis and each loaded sample had 5  $\mu$ L of Gel Loading Dye, Purple (6X), no SDS (Catalog # B7025S) per 25  $\mu$ L reaction volume. The DNA and loading dye mixture were mixed well on Parafilm before being loaded into the desired well in the agarose gel. Once the desired amount of DNA was loaded into the agarose gel wells, including the ladder, the current was started at 100 Volts and ran for approximately 45 to 95 minutes depending on the tracking of the red band generated by the purple load dye. The red band tracks through the 1% agarose gel as a piece of DNA with approximate length of 300 base pairs. This was important for direction, speed of travel, and to determine time run time for proper separation of different sized bands. This same method was employed for DNA band isolation for determining digested and undigested plasmid DNA. To determine the DNA amounts gel quantification was applied to either verify the concentration determined by the NanoSpec or used as a stand-alone result.

### ***5.3.3 Sequencing***

Sequencing performed in this project was conducted by Retrogen Incorporated in San Diego, California. The primer used in sequencing was against the T7 tag vector sequence. The data generated by Retrogen was then imported into the SnapGene® software for alignment analysis.

#### **5.4 Resuspension of Lyophilized PN2 oligonucleotide**

Lyophilized samples of the forward and reverse PN2 oligonucleotides were ordered from Integrated DNA Technologies. When received the samples appeared translucent and were virtually undetectable to the naked eye. The samples were first centrifuged at maximum speed for 1 minute before opening the tops of their centrifuge tubes. Then concentrated stock for each were resuspended at a concentration of 100  $\mu\text{M}$  and a working stock concentration of 10  $\mu\text{M}$ ; both made with TE Buffer (10mM Tris; 0.1 mM EDTA; pH 8.0). The following oligonucleotides were generated by Integrated DNA Technologies, Inc. (Skokie, Illinois):

#### **5.5 Design of PN2**

The forward and reverse oligonucleotides were ordered with the plan to anneal them together. Thus, the annealed double stranded product would constitute the sequence for the PN2 inhibitor with overhangs matching the *Hind*III and *Eco*RI restriction sites.

### 5.5.1 PN2 forward

Sequence - PN2 forward 20 nmole Ultramer® DNA Oligo, 186 Bases

5- /5Phos/AAT TAA GCA GAA CCA CAA ACA GCC ATA CAG TAC TCC TCA  
GTG TCG AAG TTG TTT CTG TTA CCA CCA CAA CCA CCG TAG AAG AAT GGA  
GCA CAC TTA CCC TCA GTA ACG TCG AAG TAC CAT CTA GAA ATC ATA GCT  
CTA CAT GGA CCA GTC TCA GCT TGC TCA GAA CAA ACC TCT CTA ACA ACC  
TCC -3

Properties:

T<sub>m</sub> (50 nM NaCl): 70.7 °C

GC Content: 45.2%

Molecular Weight: 57016.9

nmol/OD260: 0.6

µg/OD260: 31.6

Ext. Coefficient: 1803400 L/(mole·cm)

### 5.5.2 PN2 reverse

Sequence - Pn2 reverse 20 nmole Ultramer® DNA Oligo, 186 Bases

5- /5Phos/AGC TGG AGG TTG TTA GAG AGG TTT GTT CTG AGC AAG CTG  
 AGA CTG GTC CAT GTA GAG CTA TGA TTT CTA GAT GGT ACT TCG ACG TTA  
 CTG AGG GTA AGT GTG CTC CAT TCT TCT ACG GTG GTT GTG GTG GTA ACA  
 GAA ACA ACT TCG ACA CTG AGG AGT ACT GTA TGG CTG TTT GTG GTT CTG  
 CTT -3

Properties:

T<sub>m</sub> (50 nM NaCl): 70.8 °C

GC Content: 46.2%

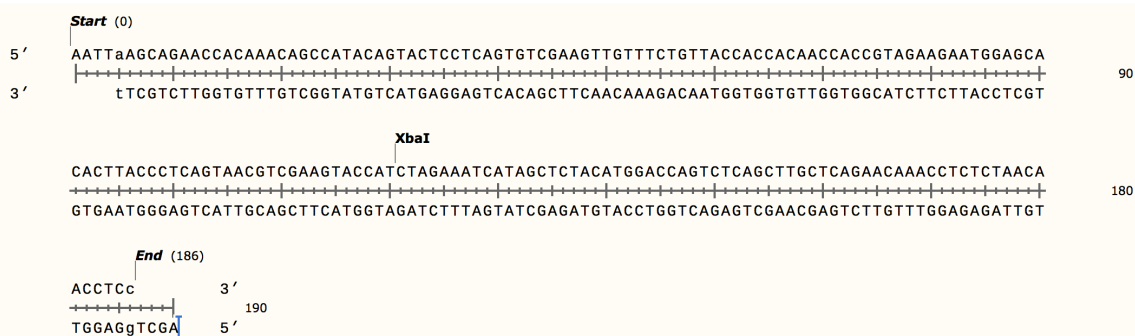
Molecular Weight: 57940.3

nmoles/OD260: 0.6

ug/OD260: 32.3

Ext. Coefficient: 1793300 L/(mole·cm)

Annealing of forward and reverse PN2-KPI primers results in following structure:



## 5.6 Restriction Digest

New England Biolabs restriction enzymes, *XbaI* (Catalog #R0145S), *NcoI-HF* (Catalog #R3193L), *HindIII-HF* (Catalog #R3104L), *EcoRI-HF* (Catalog #R3101L), and *Alkaline Phosphatase, Calf Intestinal (CIP)* (Catalog #M0290L), had incubation temperatures of 37°C in NEBuffer CutSmart buffer. All restriction enzymes could be heat inactivated at temperatures of 80°C, except for Calf Intestinal Phosphatase (CIP). Therefore, all reactions were performed in a ThermoFisher Applied Biosystems™ Veriti™ 96-Well Thermal Cycler under controlled conditions. The heat inactivation of *XbaI* was 65°C, but for the simplicity of programming 80°C was used. The reaction conditions *XbaI* (Catalog #R0145S), *NcoI-HF* (Catalog #R3193L), *HindIII-HF* (Catalog #R3104L), *EcoRI-HF* (Catalog #R3101L) were as follows:

Restriction Enzyme	20 units
DNA	Up to 1 µg
10X NEBuffer CutSmart	5 µl (1X)
Total Reaction Volume	50 µl
Incubation Time	3 hours
Incubation Temperature	37°C
Heat Inactivation Time	20 minutes
Heat Inactivation Temperature	80°C

Once the first restriction digest was completed the DNA was purified by gel electrophoresis and extracted as described. The next restriction was only heat inactivated before with the Calf Intestinal Phosphatase (CIP) treatment



The CIP treatment was performed to remove the 5'-phosphate by the addition of 20 units of CIP to the previously heat inactivated digest. The ThermoFisher Applied Biosystems™ Veriti™ 96-Well Thermal Cycler was programmed to run for 1 hour at 37°C to allow the phosphatase to cleave. Afterwards, the temperature dropped in the ThermoFisher Applied Biosystems™ Veriti™ 96-Well Thermal Cycler to 4°C until removed. After the CIP treatment, a Phenol-Chloroform-Isoamyl Extraction with Ethanol precipitation to stop the phosphatase was performed.

## **5.7 Purification**

### **5.7.1 Phenol-Chloroform-Isoamyl Extraction**

To remove the restriction enzymes and ensure that the DNA is free of proteins and lipids it is essential to perform an extraction. Once the extraction is performed the purified DNA is then able to be used in the next phase of the experiment. The DNA mixture was mixed with one volume of phenol:chloroform:isoamyl alcohol in a ratio of 25:24:1, respectively. The solution was then vortexed thoroughly for approximately 20 to 30 seconds, followed by centrifugation at room temperature for 2 minutes at 13,300 x g. Next, the upper aqueous layer was removed and transferred to a fresh tube, being careful to not get phenol during pipetting. To ensure the removal of all phenol another wash was performed with equal volume of chloroform, then vortexed for approximately 20 to 30 seconds, followed by centrifuging at room temperature for 2 minutes at 13,300 x g. The upper aqueous layer was transferred to a fresh tube for ethanol precipitation.

### **5.7.2 Ethanol Precipitation**

The microcentrifuge tube containing the DNA solution had 3M Sodium Acetate added at 1/10 volume, then vortexed to ensure mixture of salt with DNA. Next, 2X volume ice-cold 100% Ethanol was added and vortexed to provide a complete mixture. The mixture was placed in -80°C for at least 1 hour but typically left overnight. When the mixture was removed, the mixture was centrifuged at 13,300 x *g* for 20 minutes at 4°C. The supernatant was then decanted carefully to not disturb the pellet. Next, the pellet was washed with 70% ice-cold ethanol and allowed to stand at room temperature for 5 minutes. The tube was then centrifuged again at 13,300 x *g* for 20 minutes at 4°C, and the supernatant was removed by pipetting. The pellet was then air dried for approximately 20 to 30 minutes or until no trace smell of ethanol existed. The dried pellet was then resuspended with 20-40 µL Nuclease-free water or 1X TE buffer via gently pipetting. The resuspension was incubated at 37°C for 15 to 20 minutes to ensure resuspension.

## 5.8 Ligation

New England Biolabs T4 DNA Ligase (400,000 cohesive end units/ml; Catalog # M0202L) was used in all ligations. The protocol was set up as follows:

Vector DNA	1.000x10 <sup>-5</sup> -2.000x10 <sup>-5</sup> nmol
Insert DNA	3.000x10 <sup>-5</sup> -5.000x10 <sup>-5</sup> nmol
T4 DNA Ligase	400 Units
T4 DNA 10X Ligase Buffer	2µl
Nuclease-free water	Up to 20 µl
Total Reaction Volume	20µl

Vector DNA to Insert DNA was set up at a 1:3 or 1:6 molar ratio. This reaction was set up on ice and the T4 ligase added last. The reaction was placed in the ThermoFisher Applied Biosystems™ Veriti™ 96-Well Thermal Cycler for 14 hours at 16°C. The reaction was stored in the 4°C refrigerator or on ice until used in the transfection.

## 5.9 Polymerase Chain Reaction

The following PCR primers generated by Integrated DNA Technologies, Inc. (Skokie, Illinois) were used for sub-cloning the original insert with the restriction sites in a different reading frame orientation.

### 5.9.1 Primer #1: HindIII replacing NcoI-NT

The 34 Bases of Sequence - HindIII replacing NcoI-NT were 5'- ATA CAA AGC TTC ATG GGC TAC CAC CAC CAC CTT T -3'. Properties of the designed primer sequence were:

T<sub>m</sub> (50 nM NaCl): 65.2 °C

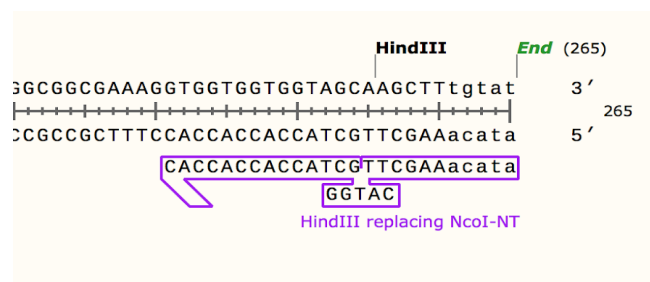
GC Content: 47.1%

Molecular Weight: 10290.7

nmoles/OD260: 3.1

ug/OD260: 32.4

Ext. Coefficient: 317900 L/(mole·cm)



### 5.9.2 Primer #2: NcoI Replacing HindIII-OT

The 42 bases of Sequence - NcoI Replacing HindIII-OT were 5'- ACA CCA TGG AGC TTA TGA AAA CCA AAA ACT TTC TTC TTT TTT -3'. Properties of the designed primer were:

T<sub>m</sub> (50 nM NaCl): 61.9 °C

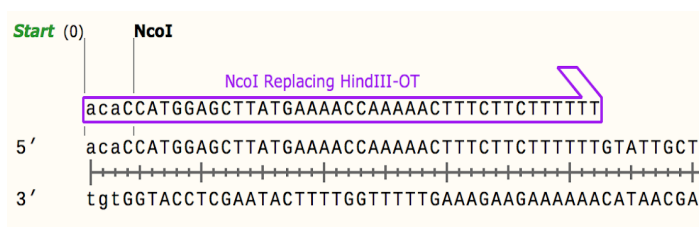
GC Content: 31%

Molecular Weight: 12805.4

nmoles/OD260: 2.5

ug/OD260: 31.9

Ext. Coefficient: 400800 L/(mole·cm)



The oligonucleotides were resuspended in TE buffer (10mM Tris; 0.1 mM EDTA; pH 8.0) with a 100 µM concentrated resuspension and a 10 µM working stock working stock concentration

The Polymerase Chain Reaction mixture was set up as follows using the Q5<sup>®</sup> HF polymerase kit (New England Biolabs; Catalog # M0492S).

	Final Concentration
Q5 HF Master Mix 2X	1X
10 $\mu$ M of Primer #1: HindIII replace NcoI-NT	0.5 $\mu$ M
10 $\mu$ M of Primer #2: NcoI replace HindIII-OT	0.5 $\mu$ M
PLE10 Template DNA	1 pg
Nuclease-Free Water	Up to 50 $\mu$ L
Total Volume	50 $\mu$ L

This mixture was placed in a PCR reaction tube. The ThermoFisher Applied Biosystems<sup>™</sup> Veriti<sup>™</sup> 96-Well Thermal Cycler ran using the program NPB Q5 HF method 2, which was programmed as follows:

Step	Temperature ( $^{\circ}$ C)	Time (seconds)
Denaturation	98	30
35 cycles	98	10
	72	60
Final Extension	72	120
Hold	4	$\infty$

Once the PCR was completed the PCR tubes were pooled and placed in 4 °C refrigerator. Analysis of the PCR product was performed with the NanoSpec to determine DNA concentration of the PCR products.

### ***5.10 DNA extraction from Agarose Gels***

QIAEX II® Gel Extraction Kit (Qiagen; Hilden, Germany; Catalog # 20021) was used to harvest DNA from agarose gels. The manufacturer's protocol was followed but modified to fit specific requirements.

DNA product was loaded into the well of a 1% TAE agarose gel that was contained in a Gel Electrophoresis Chamber and electrophoresed at 100 volts for roughly 60 minutes. The 1% TAE agarose gel, containing electrophoresed DNA product, was imaged with an UV gel imager. The individual bands were excised while under UV light to determine precise location using a sharp scalpel blade. If DNA banding patterns were not clearly distinct to separate based on size compared to the NEB Quick-Load 2-Log DNA Ladder and other DNA products in same lane, then the gel was placed back into the Gel Electrophoresis Chamber in 10-minute increments until optimal separation was obtained. To maximize the recovery all agarose lacking DNA was removed from the excised band, so the weight of agarose was approximately 250 mg. The agarose containing DNA was placed in an empty, pre-weighed 2 ml microcentrifuge tube, and weighed to determine mass. Next, 2 volumes of Buffer QX1, 2 volumes of nuclease-free H<sub>2</sub>O, and 30 µl of QIAEX II solution were added to 2 ml microcentrifuge tube. The QIAEX II solution was vortexed exceptionally well to ensure proper mixture before

adding to the buffer containing the agarose. After addition of QIAEX II, the solution was incubated at 65°C for 12 minutes, and vortexed every 2 minutes. Intermittent vortexing allowed proper binding of QIAEX II to the DNA. Next, the solution was centrifuged for 30 seconds at maximum speed, and the supernatant was removed with a pipet. A pellet wash was performed with 500 µl of Buffer QX1 and vortexed to resuspend the pellet. The supernatant was pipetted and discarded after a 30-second centrifuge. Next, the pellet was washed twice with 500 µl of Buffer PE. For each wash, the pellet was vortexed to resuspend in solution, then centrifuged to pellet the QIAEX II beads and supernatant was removed. After final wash was completed, the pellet was air dried for 30 minutes or until the pellet was white. With a dry white pellet, the DNA was eluted with 40 µl of nuclease-free H<sub>2</sub>O, vortexed the pellet to resuspend, and incubated at 70°C for 15 minutes. The resuspended pellet was stirred with a pipet tip and incubated an additional 5 minutes. The DNA yield was increased by a final maximum speed centrifugation that lasted a minimum of 30 seconds, but less than 45 seconds. This last step eluted additional DNA into the nuclease-free water. Next the nuclease-free water that contained eluted DNA was pipetted into a new centrifuge tube.



## 6 Results

### 6.1 Dissection of pET11D

*E. coli* DH5 $\alpha$  was chosen as a plasmid maintenance host of pET11D. Figure 7 demonstrates a vector map of the pET11d plasmid isolated from the bacterial cell. The plasmid contains multiple restriction sites that were selected based on location and orientation to the ribosome binding site (RBS) and the open reading frame (ORF).

The gene encoding LAGC-(EAAAK)<sub>11</sub>, to be named AMR, was previously cloned into the pET11d plasmid and was gifted from a former Georgia Campus – Philadelphia College of Osteopathic Medicine Thesis Student, Robin Conley (83). The Apyrase leader sequence directs translocation of the LAGC sequence from the cytosol to the periplasmic space of the *E. coli* and is then cleaved by the cellular machinery. The LAGC, a portion of the lipobox protein, serves as a signal sequence that is cleaved, then modified with an N-acetyl moiety. Each EAAAK motif forms a rigid alpha helical structure which will extend

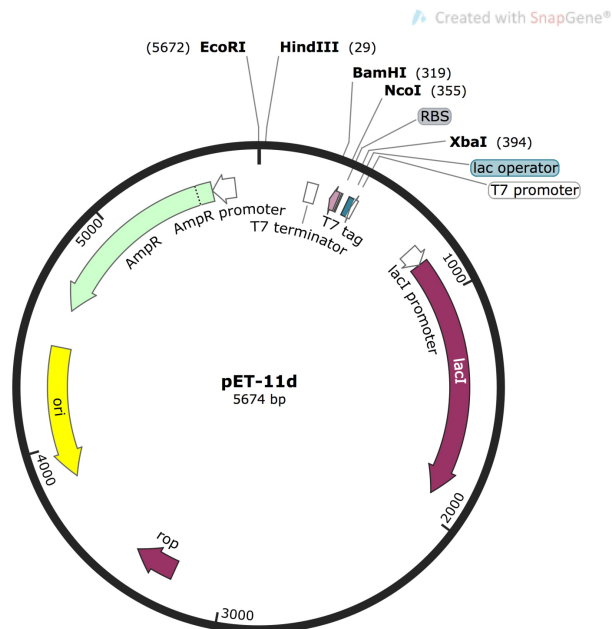


**Figure 7** pET-11d Vector Map with a length of 6,674 base pairs. The restriction sites used are identified with names and locations on the vector. Also noted is the Open Reading Frame direction and location of the Ampicillin Resistance Gene.

from the N-acyl-S-diacylglycerylcysteine lipid anchor moiety. To achieve the desired distance between the inhibitor moiety and the phospholipid anchor, the EAAAK motif was repeated a total of eleven times. Encoded at the terminus of the EAAAK region is a GGGGS flexible linker sequence. The flexible nature of GGGGS allows for the mobility of the inhibitor, instead of being directly tethered to the rigid EAAAK sequence

## 6.2 PCR Reorientation and Purification of AMR

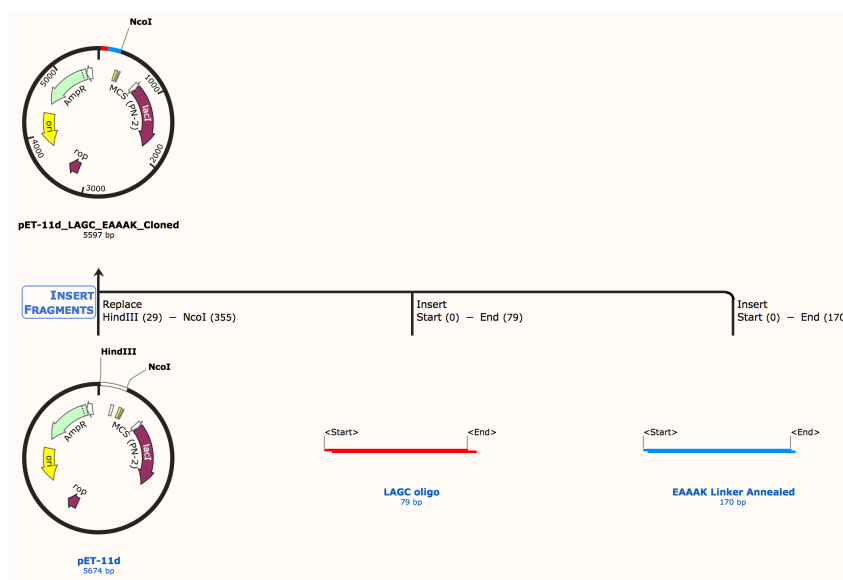


**Figure 8** pET-11d Vector Map with the LAGC-EAAAK sequence inherited from a previous student.. The restriction sites used are identified with names and locations on the vector. Also noted is the Open Reading Frame direction and location of the Ampicillin Resistance Gene.

The gifted plasmid, p-LAGC-EAK11, contained the *Shigella* apyrase leader sequence, anchor sequence LAGC, repeated ruler sequence EAAAK and flexible linker sequence GGGGS inserted between restriction sites *NcoI* and *HindIII* (see Figure 8).

Employing the p-LAGC-EAK11 plasmid as the cloning backbone for the PN2 inhibitor, in-depth analysis determined the reading frame directionality was incorrect. Correct placement of AMR sequence is necessary for not only protein expression but for the addition of the PN2-KPI inhibitor.

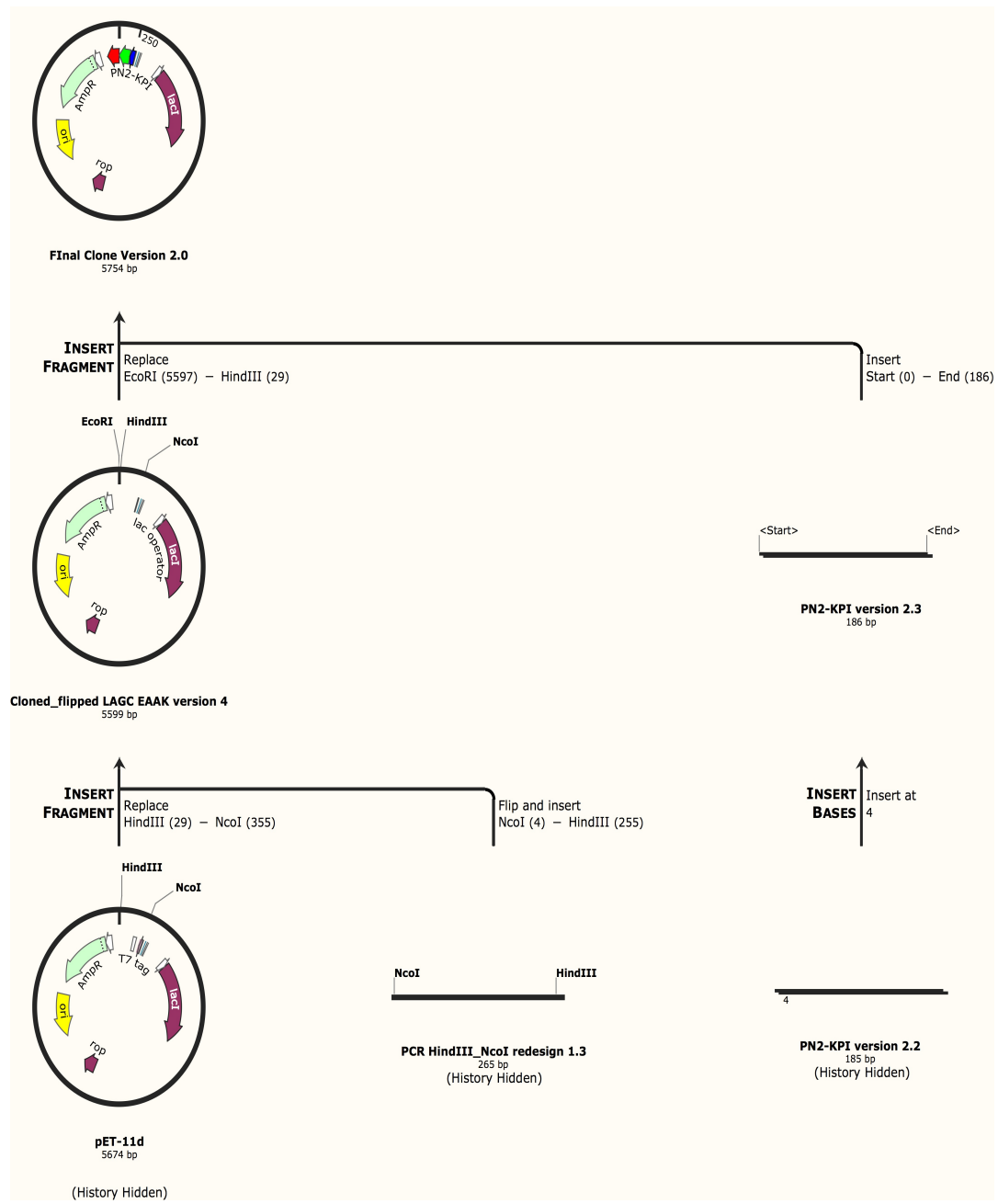


**Figure 9** Master Plan Overall View. Correction of pET-11d Vector with the LAGC-EAAK (AMR) sequence inherited from a previous student. Redesign of the PN2-KPI and insertion into the vector to produce the final product, AMRI. The restriction sites used are identified with names and locations on the vector. Also noted is the Open Reading Frame direction and location of the Ampicillin Resistance Gene.

A master plan (see Figure 9) was developed to use PCR to re-engineer the restriction sites and correct the AMR reading frame orientation by subcloning out the previous bits and swapping their orientation before adding the PN2-KPI sequence. The new reverse strand, named 'HindIII replacing NcoI-NT', and the new forward strand, named 'NcoI replacing HindIII-OT' were used to re-engineer the orientation of the strand. Following the PCR, the entire AMR sequence underwent a double digest with HindIII and NcoI. Upon completion of the restriction digest, a Phenol/Chloroform extraction was performed to purify the AMR product. Gel electrophoresis (See Figure 10) and was performed on the AMR product to ensure size of the product. Once confirmed that the product was of desired size the process was repeated on a larger scale and gel analysis had a concentration of 725 ng Restricted Flipped Insert used in the gel analysis (see Figure 10). The NanoSpec reading on the total collected volume was 6640 ng total of AMR insert from the PCR reaction.

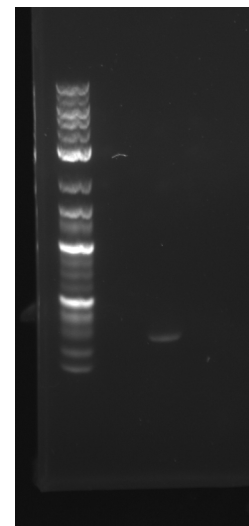


**Figure 10**

Confirmation of AMR PCR product. The expected band size is 356 base pairs.

### **6.3 Purification of Restricted pET11d Plasmid**

Generation of new *E.coli* DH5 $\alpha$  containing the pET11d plasmid was performed to have ample stock for the pET11d-AMR ligation reaction. For the generation of sticky ends, the pET11d vector was restricted with NcoI in the thermocycler for 3 hours at 37°C, followed by heat inactivation at 80°C for 20 minutes, and held at 4°C until removal

from thermocycler. A 1% agarose gel containing Phenix Red was the standard for all gel purifications with the bands excised under UV light, and plasmid DNA harvested via QIAEX-II gel extraction kit (see Figure 11).

When using the gel extraction kit, following the manufacturer's protocol except for the heat recommendation, a heat setting of 65°C to 70°C was found to be optimal for extraction of DNA from the QIAEX-II beads. The NanoSpec then quantified the NcoI\_pET11d plasmid concentrations to ensure both quantity and quality.

pET11d\_NcoI plasmid was then restricted with HindIII for 2 hours in the thermocycler, heat inactivated at 80°, and held at 4°C. The pET11d\_NcoI\_HindIII plasmid was CIP treated at 37°C in the thermocycler for 1 hour. Purified pET11d\_NcoI\_HindIII\_CIP was obtained by two phenol/chloroform extraction and single ethanol precipitation. Quantification was performed using the NanoSpec reading to generate the total 180.4 ng of DNA.

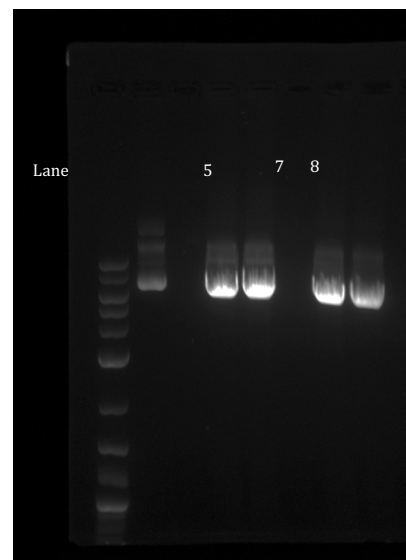


**Figure 11 pET-11d Restriction. In lanes 4 and 5 the plasmid has been digested with HindIII, lanes 7 and 8 have been digested with NcoI. Based on the band size an estimated concentration of 600 ng per lane of DNA.**

## 6.4 Insertion and Transformation of AMR Insert

The importance of molar ratios comes into account for ligation reactions to occur between pET11d\_NcoI\_HindIII\_CIP and AMR. The ligation was performed overnight at a 1:3 vector to insert ratio at 16°C in the thermocycler. At the completion of ligation, a transformation was setup using competent *E. coli* DH5α cells, a gift from a former GA-PCOM pharmacy student, Betty Ma. To the competent cells, 10 ng of

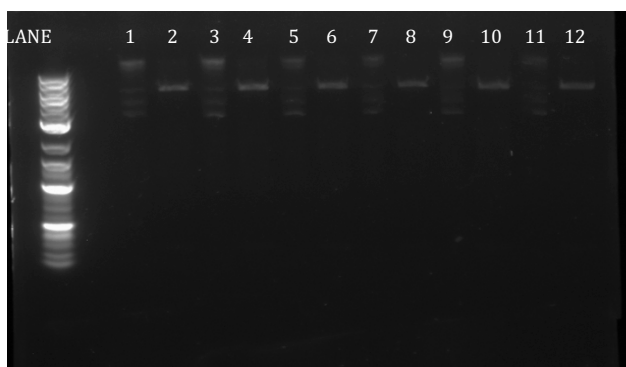


**Figure 13 Gel Electrophoresis Image of double digested Transformation Product.** The Miniprep harvested plasmid was double digested with NcoI and HindIII as confirmation before sending samples for sequencing analysis. The double digest plasmid has an expected size of 5,348 base pairs. Quick-Load 2-Log DNA Ladder (New England BioLabs, Ipswich, Massachusetts, Catalog # N0550S) was employed for size analysis.



**Figure 12 Transformation of p\_AMR into *E. coli* DH5α.** The colonies were identified and circled so that origin could be traced in detail before Miniprep was performed to send the plasmid DNA for analysis.

plasmid was pipetted into them, heat shocked at 42°C for 30 seconds, thus allowing the DNA to be transformed into the *E. coli* cells. The cell cultures were grown overnight at 37°C and colonies were observed (See Figure 12). Selections were made from the chosen colonies and inoculated into 5 ml LB broth with 50 μg/mL ampicillin and grown overnight. Midiprep was performed the following day. To

confirm the ligation and transformation a success a double digest with NcoI and HindIII on the harvested P\_AMR plasmid was performed with the restricted plasmid being 5,348 bp and the fragment 251 bp (See Figure 13). The harvested plasmids were sent to Retrogen for sequencing from the T7 (See Appendix A). A positive colony, named P1CB1, was chosen as the Gold Stock colony for all future P\_AMR plasmids due to its complete sequence.

### **6.5 Annealing and Purification of PN2-KPI**

The PN2-KPI inhibitor was annealed by mixing in equal concentrations of oligo and heating to 94°C for 2 minutes, followed by slowly cooling to room temperature. A small amount was then used to run for analysis and quantification of product.

### **6.6 Harvest of P\_AMR for use in Transformation**

P\_AMR was then harvested from *E.coli* to be used for a series of restrictions before the ligation of the PN2. The first restriction was with EcoRI as previously performed with HindIII, followed by gel purification, and QIAEX-II gel extraction. NanoSpec quantification and gel verification was used to ensure full linearization before proceeding to the restriction with HindIII. Next, was a restriction of P\_AMR\_EcoRI with HindIII for 2 hours was performed in the thermocycler at 37°C, followed by heat inactivation at 80°C for 20 minutes. The p\_AMR\_EcoRI\_HindIII was then treated with CIP for 1 hour at 37°C. To purify p\_AMR\_EcoRI\_HindIII\_CIP a phenol/chloroform/isoamyl extraction followed by ethanol precipitation, to ensure purity of the restricted DNA. A quantification gel was used to determine the concentration of plasmid DNA after completion of purification.



## 6.7 Ligation and Transformation of p-AMR with PN2-KPI

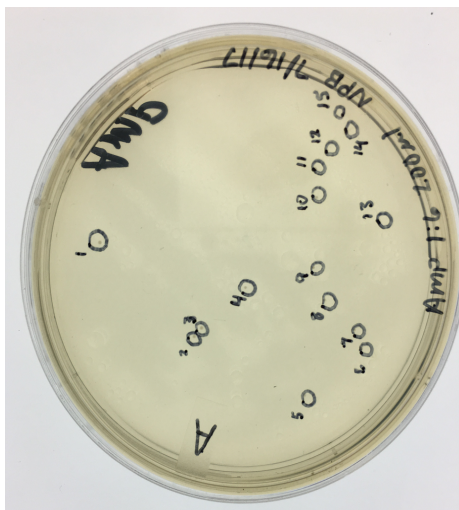


**Figure 14** Image of Transformation colony selection of p\_AMRI plasmid in *E. coli* DH5α. Isolated colonies were selected for inoculation to grow culture for sequence confirmation.

in the thermocycler overnight at 16°C and used in a transformation into competent *E. coli* DH5α cells. The chosen colonies (See Figure 14) were grown in 5 ml LB broth with 5 µg/mL ampicillin overnight, and a miniprep was used to harvest the plasmid DNA.

To ensure the confirmation of the P\_AMRI product, a restriction with *Xba*I resulted in the expected ejection of a 356 base pair fragment (See Figure 15). After restriction

A ligation reaction was set up between p\_AMR\_EcoRI\_HindIII\_CIP and PN2 insert at a molar ratio of 1:3 and 1:6. This reaction was placed

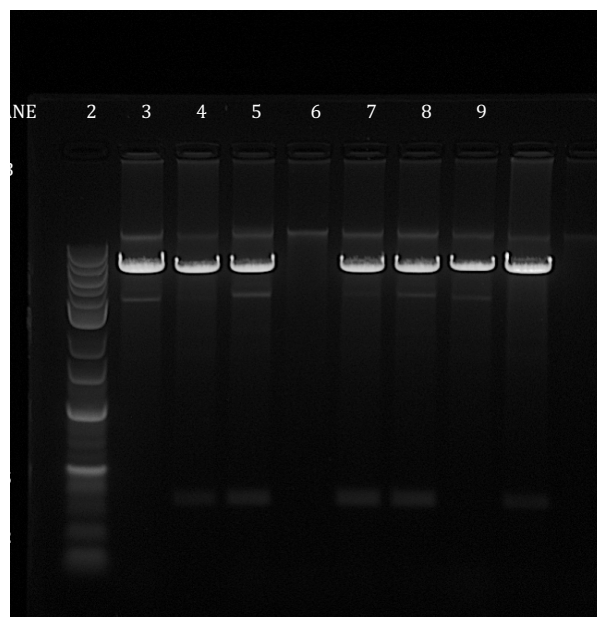


**Figure 15** Gel Confirmation of desired p\_AMRI product. The plasmid was digested with *Xba*I. On the engineered p\_AMRI *Xba*I has 2 different restriction sites in the cloned sequence, which ejected a fragment of 356 base pairs in length. Quick-Load 2-Log DNA Ladder (New England BioLabs, Ipswich, Massachusetts, Catalog # N0550S)

confirmation, the p\_AMRI plasmid was sent to Retrogen for sequencing analysis (See Appendix B).

## 7 Discussion

The goal of this study was to design and generate a lipid **Anchored Molecular Ruler with attached Inhibitor (AMRI)** at a fixed height to quantify the optimum reactive height for FIXa (see Figure 16). Having a hypothesized reactive height is between 50 to 100Å above the membrane it is important to create AMRI to fluid data and understanding of Serine Proteases, specifically for this study FIXa. This was carried out by creation, purification, and sequencing of an AMRI in an expression vector.

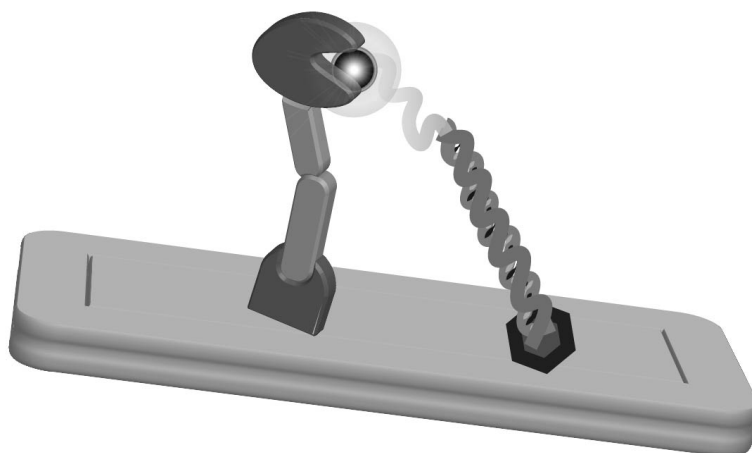


**Figure 16. Hypothesized Action of AMRI interaction with FIXa on a phospholipid surface. Here it can be seen how the AMRI (figure on left) gets the right height and the flexible linker allows the inhibitor to fit in the reactive site of FIXa (structure on the left)**

Previous studies have demonstrated the use of a variable length peptide linker and a membrane bound inhibitor. The understandings of previous FRET studies delivered great insight into a topographical orientation of the enzymes. Using the FRET data allowed for height estimation of FIXa on a phospholipid surface, but it could not necessarily correlate with the optimal reactive height, nor elasticity of the active site of the enzyme when exhibiting maximum pro-coagulant activity. This study focused on the

generation of a lipid-tethered inhibitor for use as a molecular ruler of FIXa through a successful engineering and multi-step cloning process.

The p-LAGC-EAK10 plasmid underwent a restriction digest with Restriction endonucleases, *HindIII* and *NcoI*, to produce a DNA fragment containing the LAGC and (EAAAK)<sub>11</sub> coding sequences. Using the molecular biology program, SnapGene, PCR primers were designed to mutagenize the ends, inserting *HindIII* and *NcoI* sites opposite to their original design. This “flipped” the sequence and inserted it into the correct reading frame with the Tag7 site, coding for methionine.

Standard cloning techniques were employed to sub-clone the fragment into an empty Pet11d vector, harvested from *E. coli* DH5 $\alpha$ . PN2-KPI oligonucleotides were designed on SnapGene and generated by Integrated DNA Technologies. The PN2-KPI oligonucleotides were ordered in forward and reverse reading frames and annealed to create overhangs for alignment with their *EcoRI* and *HindIII* restriction sites. For conformation of correct annealing the product was purified using gel electrophoresis; the bands excised were roughly 187 base pairs size.

A digest of *EcoRI* and *HindIII* produced the sticky ends for insertion and ligation of annealed oligonucleotides encoding the sequence for PN2-KPI, into the constructed AMR plasmid. The DNA was purified via Gel Electrophoresis and excising the band with a product size of 5754 base pairs. The DNA was for sequencing starting at the Tag 7 promoter to ensure that the final gene product is correct.

The sequencing data (see Appendix B) demonstrate the success of generating a constructed AMRI sequence in a multi-step molecular cloning process. Successful

insertion of 11 EA<sub>3</sub>K repeats will result in the PN2-KPI inhibitor having a raised height of roughly 83 Å above the membrane surface. Ideally the height of 83 Å will prove ideal for inhibition of FIXa as crystal structures and previous FRET data have indicated that active site is between 61 – 89 Å (59, 60, 68).

## **8 Future Studies**

### **8.1 Protein expression and purification of AMRI**

#### **8.1.1 Expression of LAGC-(EAAAK)<sub>11</sub>-PN2 (AMRI)**

The construction of LAGC-(EAAAK)<sub>11</sub>-PN2 in DH5a vector described in Specific Aim 1 would be expressed in *E. coli* BL21(DE3). Carbenicillin would be used, replacing Ampicillin, since it would confer more stability with  $\beta$ -lactamases and resistance to producing satellite colonies in this expression step (82). The plasmid would confirm correct coding sequence and correct reading frame orientation if *E. coli* BL21(DE3) produces colonies. The cells would then be lysed, as expressed proteins would be anchored in *E. coli* periplasmic space, with a zwitterionic detergent and would remain in detergent. Using the detergent would provide a suitable environment for the protein, since typically its lipid bound.

#### **8.1.2 Affinity Column Purification of LAGC-(EAAAK)<sub>11</sub>-PN2 (AMRI)**

##### **Crude Cell Lysate**

Purification of LAGC-(EAAAK)<sub>11</sub>-PN2 Crude Cell Lysate would be performed by Affinity Column Purification in 20 mM Tris-HCl, pH 7.5, 100 mM NaCl. The Affinity column would be generated using Affi-Gel generating an amide bond to Trypsin. The desired amount of Affi-Gel would be transferred into a funnel to separate and drain the supernatant. The gel would then be washed three times with gel bed volumes of cold 10 mM Sodium Acetate, pH 4.5. Gel is transferred to a flask and the cold Trypsin solution is added at 0.5 ml per ml of gel, followed by one hour of gentle agitation at room

temperature. Once completed the gel with trypsin would be transferred to a column and washed with water until column runs clear at O.D.<sub>280</sub>. The column was chosen since Trypsin would bind with PN2-KPI attached at the end of the folded protein. The column would be developed using an Equilibration Buffer of 20 mM Tris-HCl, pH 7.5, 100 mM NaCl, 0.1% Triton-X100 with a flow rate of approximately 1 mL per 2.5 minute. The cell lysate would then be loaded at a rate of approximately 1 mL per 2.5 minute. The cell lysate would then be eluted with 10 mM HCl, 500 mM KCl, 0.1% Triton-X100, pH 2 at a rate of 1 ml/min and fractions collected. Elutions would then be neutralized by adding 20  $\mu$ l of 1M Tris-HCl, pH 7.5, as collected. Elution fractions would then be analyzed at A<sub>280</sub> and relevant fractions would be pooled. The column would be stored at 4°C and in the starting buffer that contains 0.2% Sodium Azide (Unpublished protocol K. Baker).

### **8.1.3 Re-lipidation of LAGC-(EAAAK)<sub>11</sub>-PN2 (AMRI)**

For proper expression of AMRI, re-lipidation must occur on a phospholipid surface such as a liposome, this protocol has been adapted from Smith and Morrissey 2004 (84). These liposomes would form as the detergent is removed from, creating a layer for AMRI to effectively sit along with FIXa. Using the A<sub>280</sub> readings for estimated protein concentration it would place in a ratio of 300 nM protein with 2.6  $\mu$ M Phosphatidylcholine (PC) lipid. The mixture would then be dried under Argon gas followed by continued drying under a vacuum. The protein solution still in the elution buffer would be added to solubilize the lipids. Detergent would be removed by adding 50 mg wet SM-2 bio beads to pool the lipid vesicles. As the liposomes are forming, detergent is being removed, and the protein should re-lipidate into the liposome. After two separate 1.5-hour rocking

events the liquid around the beads would be collected; with an additional 350 mg wet SM-2 bio beads added after first rocking.

#### **8.1.4 Gel Filtration Chromatography**

Gel Filtration Chromatography would be employed using a 16 ml sepharose CL 2B 300 column at room temperature. The column would be equilibrated in a High Salt TBS, composed of 50 mM Tris-HCl, pH 7.5, 0.5 M NaCl with a running flow of 1 ml/min. The replipidated protein samples would then be added to the column and allowed to settle in column matrix. The High Salt TBS would then flow over the column at a rate of 1 ml/min and collecting fractions. The fraction turbidity would be analyzed at  $A_{600}$  to determine a lipid elution profile and proteins would be measured at  $A_{280}$ . Then proteins would be analyzed on 15% SDS-PAGE gels, followed by Silver staining using the Morrissey 1981 protocol (85). This step would confirm the proteins are fixating to the lipid membrane and not generating protein null liposomes. Proteins that are not bound to the liposome would elute early as they are small, and the lipids would elute in later fractions. If the proteins bind with the lipid they would elute in the same fractions.

#### **8.1.5 Anticipated Results**

I anticipate the engineering of the protein was correct and would produce a valid product. Expression of the protein should be accomplished because the DNA sequence is in the correct reading frame inducible under the IPTG. Isolation of the protein would be possible as well because of Trypsin and its affinity for binding.



### ***8.1.6 Potential Problems and Alternative Strategies***

Potential problems may arise in the extraction method with the detergent. The detergent is essential in lysing the cells and providing soluble protein environment. Adjustments would be made at each step and evaluated, since this protocol was adapted from the purification of BPTI. The previous protocol also lacked the larger rigid and flexible linker regions, which could affect how the inhibitor folds and behaves.

## **8.2 Determine ability of AMRI to inhibit FIXa**

### **8.2.1 Protocol**

To study reactive height of FIX, AMRI was incorporated into a liposome as described in specific Aim 2. The liposomes would be constructed of 2 anionic phospholipids, phosphatidylserine, and phosphatidylcholine (PS and PC). Their concentrations would be at 10% PS and 90% PC and should be able to promote optimal binding. It has been demonstrated with their ability to bind Vitamin K-dependent clotting factors, which contain the N-terminal  $\gamma$ -carboxyglutamic acid (Gla) domain (9, 86). Once the liposome bound with AMRI is dried to a 96- well plate activated FIXa would be added. FIXa has been previously activated by Russell's Viper Venom and stored frozen until needed. Chromogenic substrate would be added and monitored at 405 nm to determine the amount of active enzyme that remain unbound by the inhibitor, modified from Neuenschwander et al. 2006 and Yu et al. 2014 (56, 87). Rates would be plotted against inhibitor concentration to determine the  $K_i$  for AMRI.

### **8.2.2 Anticipated Results**

I anticipate that AMRI would inhibit FIXa at the height hypothesized of using the (EAAAK)<sub>11</sub> insert between the LAGC anchor and PN2-KPI.

### **8.2.3 Potential Problems and Alternative Strategies**

A potential problem is the sequence of repeats may alter the binding ability of KPI to block the catalytic triad, therefore, to test this ability a mixture of inhibitor and substrate could be placed in solution. If no reaction or weak reaction, this would be conclusive that AMRI is ineffective in a FIXa topography study. It is also possible the inhibitor could

be raised to an ineffective height; if weak inhibition then alternative repeats of EAAAK could be used to determine the optimal height of FIX. This would require multiple cloning experiments to adjust the EAAAK sequence repeats. Also, an issue that may be encountered is either FIX or inhibitor does not anchor to the phospholipid for correct positioning. If this is the case, then alternative concentration ratios of PS:PC could be used to see if a different concentration as a greater anchoring affect.

## 9 *Clinical Significance*

An abnormal blood clot forms in the blood vessel, called a thrombus. This thrombus is the result of a clinical abnormality causing activation of the clotting cascade. If the resulting thrombus moves in the vasculature, it is termed an embolus. An embolus becomes dangerous as it travels and lodges in the narrowing of the vessel, restricting or terminating blood flow.

Current medical treatment for a patient receiving a stent or angioplasty involves multiple preparation steps to ensure the patient does not develop an embolus. The current medical intervention relies heavily on drugs that interfere with the clotting cascade. Patients going in for stent placement are given a  $\text{Ca}^{2+}$  channel antagonist and injections of heparin during the procedure. Once the procedure is completed the use of heparin and coumarin (i.e. Warfarin) are continued for 72 hours. Following the 72 hours treatment with the coumarin is done for an indefinite amount of time, depending on the patients clotting times (88) .

The hope of this study of pro-coagulant enzyme/membrane topography is to bridge the knowledge gap by studying the distances of fully pro-coagulant enzyme complexes. The information from this membrane-bound activity study could lead to the generation of inhibitors with an increased specificity. Not only targeting enzyme reactivity but one directed to specific membrane topography of each enzyme. Therefore, the results of a study with AMRI could greatly impact clinical therapies aimed at coagulation reaction

inhibition. Most importantly of the therapies impacted the most would be treatment of thrombosis, surgical procedures, and the implantation of medical devices (i.e. stents)

## References

1. Ponticos M, Partridge T, Black CM, Abraham DJ, Bou-Gharios G. Regulation of Collagen Type I in Vascular Smooth Muscle Cells by Competition between Nkx2.5 and dEF1/ZEB1. *Molecular and Cellular Biology*. 2004 July 15;24(14):6151-61.
2. Josiah N. Wilcox, Kathleen M. Smith, Stephen M. Schwartz, David Gordon. Localization of Tissue Factor in the Normal Vessel Wall and in the Atherosclerotic Plaque. *Proceedings of the National Academy of Sciences of the United States of America*. 1989 Apr 15;86(8):2839-43.
3. Drake TA, Morrissey JH, Edgington TS. Selective cellular expression of tissue factor in human tissues. Implications for disorders of hemostasis and thrombosis. *The American journal of pathology*. 1989;134(5):1087.
4. Blombäck B, Blombäck M. The molecular structure of fibrinogen. *Ann N Y Acad Sci*. 1972 Dec 08;202:77-97.
5. Esmon CT, Esmon NL, Harris KW. Complex formation between thrombin and thrombomodulin inhibits both thrombin-catalyzed fibrin formation and factor V activation. *J Biol Chem*. 1982;257(14):7944-7.
6. Adams TE, Huntington JA. Thrombin-cofactor interactions: structural insights into regulatory mechanisms. *Arterioscler Thromb Vasc Biol*. 2006 Aug;26(8):1738-45.
7. Smith RP, Higuchi DA, Broze GJ. Platelet coagulation factor XIa-inhibitor, a form of Alzheimer amyloid precursor protein. *Science*. 1990;248(4959):1126-8.
8. Heemskerk JW, Bevers EM, Lindhout T. Platelet activation and blood coagulation. *THROMBOSIS AND HAEMOSTASIS-STUTTGART*. 2002;88(2):186-94.
9. Neuenschwander P, Jesty J. A comparison of phospholipid and platelets in the activation of human. *Blood*. 1988;72(5):1761-70.
10. van Dieijen G, Van Rijn J, Govers-Riemslog JW, Hemker HC, Rosing J. Assembly of the intrinsic factor X activating complex: Interactions between factor IXa, factor VIIIa and phospholipid. *Thromb Haemost*. 1985;53:376.
11. Mertens K, Bertina RM. The contribution of Ca<sup>2+</sup> and phospholipids to the activation of human blood-coagulation Factor X by activated Factor IX. *Biochem J*. 1984;223:607-15.

12. Saulius Butenas, Cornelis van 't Veer, Kenneth G. Mann. Evaluation of the Initiation Phase of Blood Coagulation Using Ultrasensitive Assays for Serine Proteases. *Journal of Biological Chemistry*. 1997 Aug 22;272(34):21527-33.
13. Heldebrant CM, Butkowski RJ, Bajaj SP, Mann KG. The Activation of Prothrombin II. Partial Reactions, Physical And Chemical Characterization Of The Intermediates Of Activation. *J Biol Chem*. 1973;248(20):7149-63.
14. Walker RK, Krishnaswamy S. The activation of prothrombin by the prothrombinase complex. The contribution of the substrate-membrane interaction to catalysis. *J Biol Chem*. 1994 11/04;269(44):27441-50.
15. Olson ST, Shore JD. Demonstration of a two-step reaction mechanism for inhibition of alpha-thrombin by antithrombin III and identification of the step affected by heparin. *J Biol Chem*. 1982;257(24):14891-5.
16. Smith SA, Travers RJ, Morrissey JH. How it all starts: Initiation of the clotting cascade. *Critical Reviews in Biochemistry and Molecular Biology*. 2015 05;50(4):326-36.
17. Rao LV, Rapaport SI. Activation of factor VII bound to tissue factor: a key early step in the tissue factor pathway of blood coagulation. *Proceedings of the National Academy of Sciences*. 1988;85(18):6687-91.
18. Neuenschwander PF, Morrissey JH. Roles of the membrane-interactive regions of factor VIIa and tissue factor. The factor VIIa Gla domain is dispensable for binding to tissue factor but important for activation of factor X. *J Biol Chem*. 1994;269(11):8007-13.
19. Esmon CT, Jackson CM. The conversion of prothrombin to thrombin III. The factor Xa-catalyzed activation of prothrombin. *J Biol Chem*. 1974;249(24):7782-90.
20. Adams TE, Huntington JA. Structural transitions during prothrombin activation: On the importance of fragment 2. *Biochimie*. 2016 March 1;122:235-42.
21. Hoffman M. Remodeling the Blood Coagulation Cascade. *Journal of Thrombosis and Thrombolysis*. 2003 08;16(1/2):17-20.
22. Radcliffe R, Nemerson Y. Activation and control of factor VII by activated factor X and thrombin. Isolation and characterization of a single chain form of factor VII. *J Biol Chem*. 1975;250(2):388-95.
23. Hoffman M, Monroe 3rd DM, Roberts HR. Activated factor VII activates factors IX and X on the surface of activated platelets: thoughts on the mechanism of action of high-dose activated factor VII. *Blood coagulation & fibrinolysis: an international journal in haemostasis and thrombosis*. 1998;9:S61.

24. Ke Ke, Jian Yuan, James H Morrissey. Tissue Factor Residues That Putatively Interact with Membrane Phospholipids. *PLoS One*. 2014 Feb 1,;9(2):e88675.
25. Jones ME, Griffith MJ, Monroe DM, Roberts HR, Lentz BR. Comparison of lipid binding and kinetic properties of normal, variant, and. gamma.-carboxyglutamic acid modified human factor IX and factor IXa. *Biochemistry (N Y)*. 1985;24(27):8064-9.
26. Morrissey JH, Neuenschwander PF, Huang Q, McCallum CD, Su B, Johnson AE. Factor VIIa-tissue factor: functional importance of protein-membrane interactions. *Thromb Haemost*. 1997;78(01):112-6.
27. Naito K, Fujikawa K. Activation of human blood coagulation factor XI independent of factor XII. Factor XI is activated by thrombin and factor XIa in the presence of negatively charged surfaces. *J Biol Chem*. 1991;266(12):7353-8.
28. Pieters J, Lindhout T, Hemker HC. In situ-generated thrombin is the only enzyme that effectively activates factor VIII and factor V in thromboplastin-activated plasma. *Blood*. 1989;74(3):1021-4.
29. Bom VJ, Bertina RM. The contributions of Ca<sup>2+</sup>, phospholipids and tissue-factor apoprotein to the activation of human blood-coagulation factor X by activated factor VII. *Biochem J*. 1990;265(2):327-36.
30. Walker FJ, Sexton PW, Esmon CT. The inhibition of blood coagulation by activated protein C through the selective inactivation of activated factor V. *Biochimica et Biophysica Acta (BBA)-Enzymology*. 1979;571(2):333-42.
31. Esmon CT. Protein-C: biochemistry, physiology, and clinical implications. *Blood*. 1983;62(6):1155-8.
32. Bode W, Turk D, Karshikov A. The refined 1.9-Å X-ray crystal structure of D-Phe-Pro-Arg chloromethylketone-inhibited human alpha-thrombin: structure analysis, overall structure, electrostatic properties, detailed active-site geometry, and structure-function relationships. *Protein science : a publication of the Protein Society*. 1992 Apr;1(4):426-71.
33. Stone SR, Braun PJ, Hofsteenge J. Identification of regions of. alpha.-thrombin involved in its interaction with hirudin. *Biochemistry (N Y)*. 1987;26(15):4617-24.
34. van't Veer C, Golden NJ, Kalafatis M, Mann KG. Inhibitory Mechanism of the Protein C Pathway on Tissue Factor-induced Thrombin Generation Synergistic Effect In Combination With Tissue Factor Pathway Inhibitor. *J Biol Chem*. 1997;272(12):7983-94.
35. Koedam JA, Meijers JC, Sixma JJ, Bouma BN. Inactivation of human factor VIII by activated protein C. Cofactor activity of protein S and protective effect of von Willebrand factor. *J Clin Invest*. 1988;82(4):1236-43.



36. Hagen FS, Gray CL, O'Hara P, Grant FJ, Saari GC, Woodbury RG, et al. Characterization of a cDNA coding for human factor VII. *Proceedings of the National Academy of Sciences*. 1986;83(8):2412-6.
37. O'Hara PJ, Grant FJ, Haldeman BA, Gray CL, Insley MY, Hagen FS, et al. Nucleotide sequence of the gene coding for human factor VII, a vitamin K-dependent protein participating in blood coagulation. *Proceedings of the National Academy of Sciences*. 1987;84(15):5158-62.
38. Schmidt AE, Sun M, Ogawa T, Bajaj SP, Gailani D. Functional role of residue 193 (chymotrypsin numbering) in serine proteases: influence of side chain length and  $\beta$ -branching on the catalytic activity of blood coagulation factor XIa. *Biochemistry (N Y)*. 2008;47(5):1326-35.
39. Schmidt AE, Bajaj SP. Structure–Function Relationships in Factor IX and Factor IXa. *Trends in Cardiovascular Medicine*. 2003 January;13(1):39-45.
40. Badellino KO, Walsh PN. Localization of a Heparin Binding Site in the Catalytic Domain of Factor XIa . *Biochemistry*. 2001;40(25):7569-80.
41. Bode W, Brandstetter H, Mather T, Stubbs MT. Comparative analysis of haemostatic proteinases: structural aspects of thrombin, factor Xa, factor IXa and protein C. *Thromb Haemost*. 1997;78(1):501.
42. Brandstetter H, Bauer M, Huber R, Lollar P, Bode W. X-ray structure of clotting factor IXa: active site and module structure related to Xase activity and hemophilia B. *Proceedings of the National Academy of Sciences*. 1995 October 10,;92(21):9796-800.
43. Brandstetter H, Kühne A, Bode W, Huber R, von der Saal W, Wirthensohn K, et al. X-ray structure of active site-inhibited clotting factor Xa implications for drug design and substrate recognition. *J Biol Chem*. 1996;271(47):29988-92.
44. Hopfner K, Lang A, Karcher A, Sichler K, Kopetzki E, Brandstetter H, et al. Coagulation factor IXa: the relaxed conformation of Tyr99 blocks substrate binding. *Structure*. 1999 15 August;7(8):989-96.
45. Krishnaswamy S, Field KA, Edgington TS, Morrissey JH, Mann KG. Role of the membrane surface in the activation of human coagulation factor X. *J Biol Chem*. 1992;267(36):26110-20.
46. Krishnaswamy S, Church WR, Nesheim ME, Mann KG. Activation of human prothrombin by human prothrombinase. Influence of factor Va on the reaction mechanism. *J Biol Chem*. 1987;262(7):3291-9.

47. Kirchhofer D, Eigenbrot C, Lipari MT, Moran P, Peek M, Kelley RF. The Tissue Factor Region That Interacts with Factor Xa in the Activation of Factor VII. *Biochemistry*. 2001;3(40):675-82.
48. Ohkubo YZ, Morrissey JH, Tajkhorshid E. Dynamical view of membrane binding and complex formation of human factor VIIa and tissue factor. *Journal of thrombosis and haemostasis : JTH*. 2010 May;8(5):1044.
49. McCallum CD, Su B, Neuenschwander PF, Morrissey JH, Johnson AE. Tissue Factor Positions and Maintains the Factor VIIa Active Site Far above the Membrane Surface Even in the Absence of the Factor VIIa Gla Domain A FLUORESCENCE RESONANCE ENERGY TRANSFER STUDY. *J Biol Chem*. 1997;272(48):30160-6.
50. Kovalenko TA, Panteleev MA, Sveshnikova AN. The mechanisms and kinetics of initiation of blood coagulation by the extrinsic tenase complex. *Biophysics*. 2017;62(2):291-300.
51. Kovalenko TA, Panteleev MA, Sveshnikova AN. Substrate delivery mechanism and the role of membrane curvature in factor X activation by extrinsic tenase. *J Theor Biol*. 2017;435:125-33.
52. Di Scipio RG, Kurachi K, Davie EW. Activation of human factor IX (Christmas factor). *J Clin Invest*. 1978;61(6):1528.
53. ROSEMARY BIGGS, A. S DOUGLAS, M.R.C.P. R. G MACFARLANE, Radclitje I, O J. V DACIE, MCP. A CONDITION PREVIOUSLY MISTAKEN FOR HAEMOPHILIA. *Br Med J*. 1952 -12-27;2(4799):1378-82.
54. Lu, Yang, Manithody, Wang, Rezaie. Expression and Characterization of Gly-317 Variants of Factor IX Causing Variable Bleeding in Hemophilia B Patients. *Biochemistry*. 2015 06;54(24):3814-21.
55. Perot E, Enjolras N, Le Quellec S, Indalecio A, Girard J, Negrier C, et al. Expression and characterization of a novel human recombinant factor IX molecule with enhanced in vitro and in vivo clotting activity. *Thromb Res*. 2015;135(5):1017-24.
56. Neuenschwander PF, Baker-Deadmond KJ, Jones AD. Low Molecular Weight Heparin Modulates the Binding and Reactivity of Factor Xa towards Basic Pancreatic Trypsin Inhibitor: A Surface Plasmon Resonance and Kinetics Study. *Low Molecular Weight Heparin Modulates the Binding and Reactivity of Factor Xa towards Basic Pancreatic Trypsin Inhibitor: A Surface Plasmon Resonance and Kinetics Study*. 2006; 108(11), 1623.
57. Rallapalli PM, Kembball-Cook G, Tuddenham EG, Gomez K, Perkins SJ. An interactive mutation database for human coagulation factor IX provides novel insights

into the phenotypes and genetics of hemophilia B. *Journal of Thrombosis and Haemostasis*. 2013;11(7):1329–1340.

58. Neuenschwander, Williamson, Nalian, Baker-Deadmond. Heparin Modulates the 99-Loop of Factor IXa: EFFECTS ON REACTIVITY WITH ISOLATED KUNITZ-TYPE INHIBITOR DOMAINS. *Journal of Biological Chemistry*. 2006 06;281(32):23066-74.

59. McCallum, Hapak, Neuenschwander, Morrissey, Johnson. The Location of the Active Site of Blood Coagulation Factor VIIa above the Membrane Surface and Its Reorientation upon Association with Tissue Factor: A FLUORESCENCE ENERGY TRANSFER STUDY. *Journal of Biological Chemistry*. 1996 11;271(45):28168-75.

60. Mutucumarana VP, Duffy EJ, Lollar P, Johnson AE. The active site of factor IXa is located far above the membrane surface and its conformation is altered upon association with factor VIIIa. A fluorescence study. *J Biol Chem*. 1992;267(24):17012-21.

61. Björk I, Lindahl U. Mechanism of the anticoagulant action of heparin. *Mol Cell Biochem*. 1982;48(3):161-82.

62. Díez-Manglano J, Mostaza J, Pose A, Formiga F, Cepeda J, Gullón A, et al. Factors associated with discontinuing or not starting oral anticoagulant therapy in older hospitalized patients with non-valvular atrial fibrillation. *Geriatrics & Gerontology International*;0(0).

63. Whitlon DS, Sadowski JA, Suttie JW. Mechanism of coumarin action: significance of vitamin K epoxide reductase inhibition. *Biochemistry (N Y)*. 1978;17(8):1371-7.

64. Li EH, Fenton II JW, Feinman RD. The role of heparin in the thrombin-antithrombin III reaction. *Arch Biochem Biophys*. 1976;175(1):153-9.

65. Olson ST, Björk I, Shore JD. [30] Kinetic characterization of heparin-catalyzed and uncatalyzed inhibition of blood coagulation proteinases by antithrombin. In: *Methods in enzymology*. Elsevier; 1993. p. 525-59.

66. Wallace A, Rovelli G, Hofsteenge J, Stone SR. Effect of heparin on the glia-derived-nexin-thrombin interaction. *Biochem J*. 1989;257(1):191-6.

67. Neuenschwander. Exosite Occupation by Heparin Enhances the Reactivity of Blood Coagulation Factor IXa. *Biochemistry*. 2004 03;43(10):2978-86.

68. Husten EJ, Esmon CT, Johnson AE. The active site of blood coagulation factor Xa. Its distance from the phospholipid surface and its conformational sensitivity to components of the prothrombinase complex. *J Biol Chem*. 1987;262(27):12953-61.


69. Banner DW, D'arcy A, Chène C, Winkler FK, Guha A, Konigsberg WH, et al. The crystal structure of the complex of blood coagulation factor VIIa with soluble tissue factor. *Nature*. 1996;380(6569):41.
70. Schmaier AH, Dahl LD, Hasan AA, Cines DB, Bauer KA, Van Nostrand WE. Factor IXa Inhibition by Protease Nexin-2/Amyloid. beta.-Protein Precursor on Phospholipid Vesicles and Cell membranes. *Biochemistry (N Y)*. 1995;34(4):1171-8.
71. Schmaier AH, Dahl LD, Rozemuller AJ, Roos RA, Wagner SL, Chung R, et al. Protease nexin-2/amyloid beta protein precursor. A tight-binding inhibitor of coagulation factor IXa. *J Clin Invest*. 1993;92(5):2540-5.
72. Nostrand, Wagner, Suzuki, Choi, Farrow, Geddes, et al. Protease nexin-II, a potent anti-chymotrypsin, shows identity to amyloid  $\beta$ -protein precursor. *Nature*. 1989 10;341(6242):546-9.
73. Van Nostrand WE, Wagner SL, Farrow JS, Cunningham DD. Immunopurification and protease inhibitory properties of protease nexin-2/amyloid beta-protein precursor. *J Biol Chem*. 1990 June 15;265(17):9591-4.
74. Li G, Huang Z, Zhang C, Dong B, Guo R, Yue H, et al. Construction of a linker library with widely controllable flexibility for fusion protein design. *Appl Microbiol Biotechnol*. 2015:1-11.
75. Kamalakkannan S, Murugan V, Jagannadham MV, Nagaraj R, Sankaran K. Bacterial lipid modification of proteins for novel protein engineering applications. *Protein Engineering Design and Selection*. 2004 October 1;17(10):721-9.
76. Bhargava T, Datta S, Ramachandran V, Ramakrishnan R, Roy RK, Sankaran K, et al. Virulent *Shigella* codes for a soluble apyrase: identification, characterization and cloning of the gene. *Curr Sci*. 1995;68(3):293-300.
77. Arai, Ueda, Kitayama, Kamiya, Nagamune. Design of the linkers which effectively separate domains of a bifunctional fusion protein. *Protein Engineering Design and Selection*. 2001 08;14(8):529-32.
78. Marqusee S, Baldwin RL. Helix stabilization by Glu... Lys salt bridges in short peptides of de novo design. *Proceedings of the National Academy of Sciences*. 1987;84(24):8898-902.
79. Wu Y, Fan C, Li Y. Protein purification involving a unique auto-cleavage feature of a repeated EAAAK peptide. *Journal of Chromatography B*. 2009;877(31):4015-21.
80. Arai R, Wriggers W, Nishikawa Y, Nagamune T, Fujisawa T. Conformations of variably linked chimeric proteins evaluated by synchrotron X-ray small-angle scattering. *Proteins: Structure, Function, and Bioinformatics*. 2004;57(4):829–838.

81. Amet, Lee, Shen. Insertion of the Designed Helical Linker Led to Increased Expression of Tf-Based Fusion Proteins. *Pharmaceutical Research*. 2008 11;26(3):523-8.
82. Sambrook J, Russell DW, Russell DW. *Molecular cloning: a laboratory manual (3-volume set)*. Immunol. 2001;49:895-909.
83. Conley RC. Characterization of lipid-anchored inhibitor rulers as a measure of enzyme topography in coagulation enzyme factor Xa. ; 2013.
84. Smith SA, Morrissey JH. Rapid and efficient incorporation of tissue factor into liposomes. *Journal of Thrombosis and Haemostasis*. 2004;2(7):1155-62.
85. Morrissey JH. Silver stain for proteins in polyacrylamide gels: a modified procedure with enhanced uniform sensitivity. *Anal Biochem*. 1981;117(2):307-10.
86. Neuenschwander, Bianco-Fisher, Rezaie, Morrissey. Phosphatidylethanolamine augments factor VIIa-tissue factor activity: enhancement of sensitivity to phosphatidylserine. *Biochemistry*. 1995 10;34(43):13988-93.
87. Yu Y, Millar CM. Measurement of factor IX activity in plasma-derived and recombinant concentrates: insights from thrombin generation and activation-based assays. *Journal of Thrombosis and Haemostasis*. 2014;12(1):62–70.
88. Fischman DL, Leon MB, Baim DS, Schatz RA, Savage MP, Penn I, et al. A Randomized Comparison of Coronary-Stent Placement and Balloon Angioplasty in the Treatment of Coronary Artery Disease. *New England Journal of Medicine*. 1994;331(8):496-501.

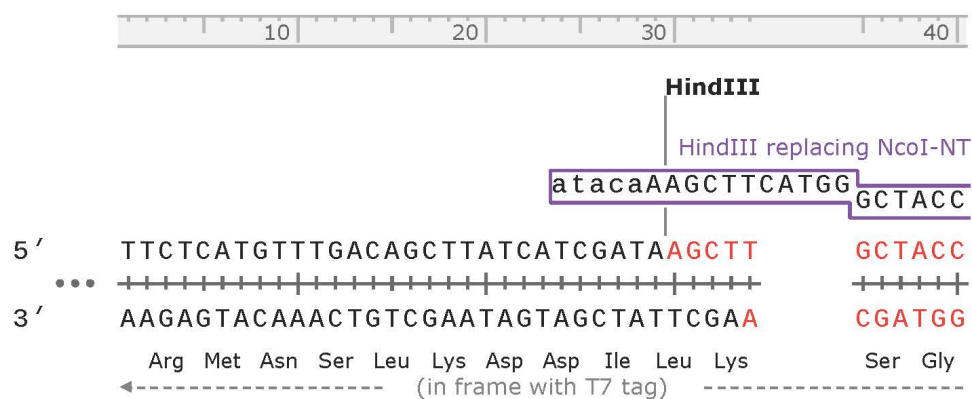
## 10 Appendices

### 10.1 Appendix A. SEQUENCE DATA IMAGES OF AMR

Cloned\_flipped LAGC EAAK version 4.dna (Circular / 5599 bp)

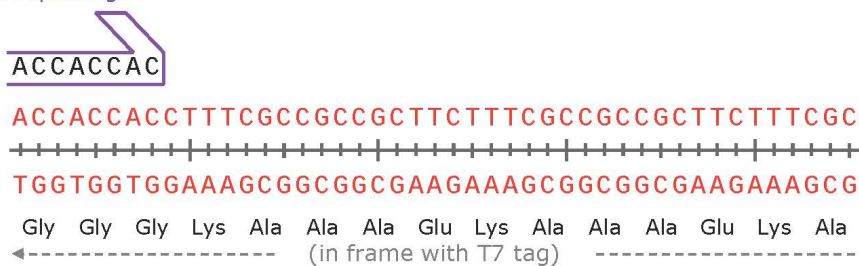
Primer	Length		Binding Sites		Tm
✓ <b>HindIII replacing...</b>	30-mer		35 .. 48		50°C
/sequence	= atacaAAGCTTCATGGGCTACCACCACCAC				
	50% GC / 9089.0 Da				
✓ <b>NcoI Replacing Hi...</b>	42-mer		247 .. 286		63°C
/sequence	= acaCCATGGAGCTTATGAAAACCAAAAACCTTCTTCTTTTT				
	31% GC / 12,805.4 Da				

Cloned\_flipped LAGC EAAK version 4.dna (Circular / 5599 bp)



50      60      70      80

HindIII replacing...



## Cloned\_flipped LAGC EAAK version 4.dna (Circular / 5599 bp)

90 | 100 | 110 | 120 | 130 |

CGCCGCTTCTTTGCGCCGCGCTTCTTTGCGCCGCGCTTCTTTTCGC  
 +-----+-----+-----+-----+-----+-----+-----+-----+-----+-----+  
 GCGGCGAAGAAAGCGGCGGCGAAGAAAGCGGCGGCGAAGAAAGCG

Ala Ala Glu Lys Ala Ala Ala Glu Lys Ala Ala Ala Glu Lys Ala  
 ←----- (in frame with T7 tag) -----

1 ← CGCCGCTTCTTTGCGCCGCGCTTCTTTGCGCCGCGCTTCTTTTCGC  
 CGCCGCTTCTTTGCGCCGCGCTTCTTTGCGCCGCGCTTCTTTTCGC

140 | 150 | 160 | 170 |

CGCCGCTTCTTTGCGCCGCGCTTCTTTGCGCCGCGCTTCTTTTCGC  
 +-----+-----+-----+-----+-----+-----+-----+-----+-----+-----+  
 GCGGCGAAGAAAGCGGCGGCGAAGAAAGCGGCGGCGAAGAAAGCG

Ala Ala Glu Lys Ala Ala Ala Glu Lys Ala Ala Ala Glu Lys Ala  
 ←----- (in frame with T7 tag) -----

1 ← CGCCGCTTCTTTGCGCCGCGCTTCTTTGCGCCGCGCTTCTTTTCGC  
 CGCCGCTTCTTTGCGCCGCGCTTCTTTGCGCCGCGCTTCTTTTCGC

180 | 190 | 200 |

CGCCGCTTCTTTGCGCCGCGCTTCTTTGCGCCGCGCTTCTTTTCGC  
 +-----+-----+-----+-----+-----+-----+-----+-----+-----+-----+  
 GCGGCGAAGAAAGCGGCGGCGAAGAAAGCGGCGGCGAAGAAAGCG

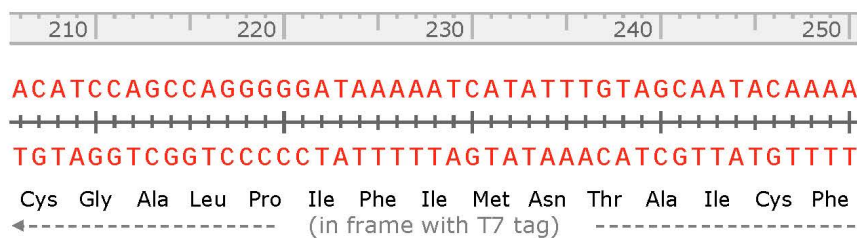
Ala Ala Glu Lys Ala Ala Ala Glu Ser Gly  
 ←----- (in frame with T7 tag) -----

**BamHI**  
 |  
 GGATCC  
 +-----+  
 CCTAGG

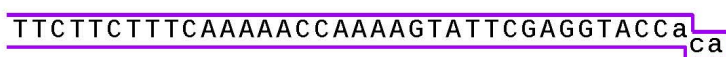
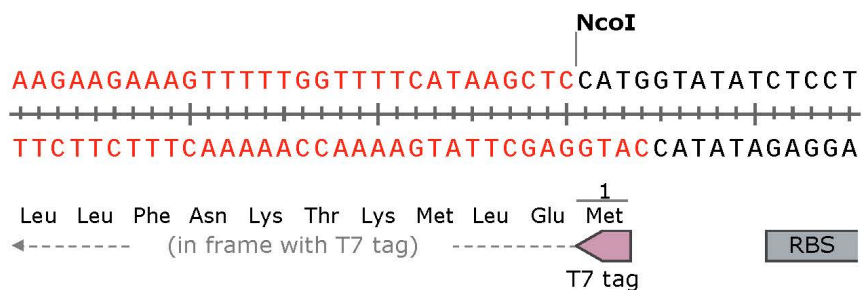
1 ← CGCCGCTTCTTTGCGCCGCGCTTCTTTGCGCCGCGCTTCTTTTCGC GGATCC  
 CGCCGCTTCTTTGCGCCGCGCTTCTTTGCGCCGCGCTTCTTTTCGC GGATCC



Cloned\_flipped LAGC EAAK version 4.dna (Circular / 5599 bp)



NcoI Replacing HindIII-OT



NcoI Replacing HindIII-OT






## 10.2 Appendix B. SEQUENCE DATA IMAGES OF AMRI

Final Clone Version 2.1\_AMRI\_alignment.dna (Circular / 5754 bp)

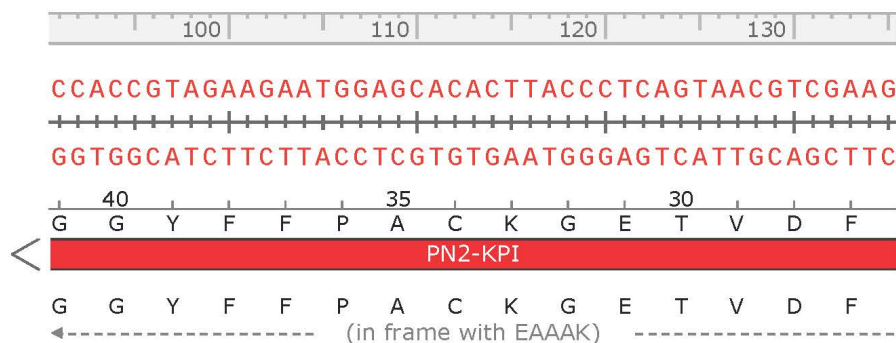
---

### Original Sequence:

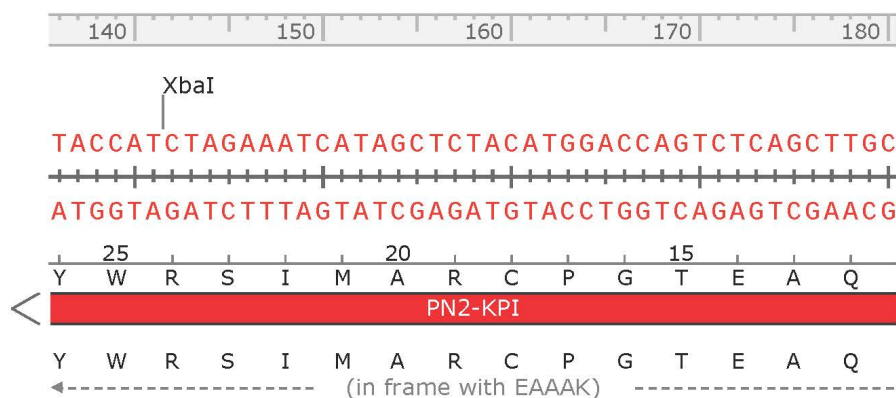
- 1: P-AMRI-A4\_T7   
1258 bases  
1 .. 1252 (54 mismatches, 12 gaps)
- 2: P-AMRI-A9\_T7   
1265 bases  
1 .. 1251 (62 mismatches, 6 gaps)
- 3: P-AMRI-B2\_T7   
1256 bases  
24 .. 1256 (29 mismatches, 3 gaps)



Final Clone Version 2.1\_AMRI\_alignment.dna (Circular / 5754 bp)

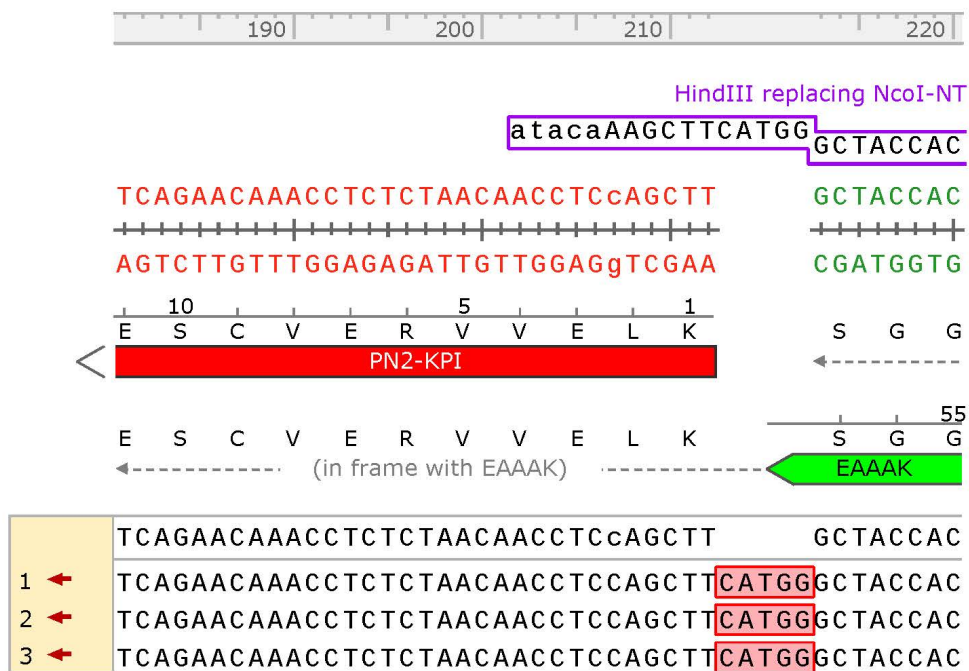


	CCACCGTAGAAGAATGGAGCACACTTACCCTCAGTAACGTCGAAG
1 ←	CCACCGTAGAAGAATGGAGCACACTTACCCTCAGTAACGTCGAAG
2 ←	CCACCGTAGAAGAATGGAGCACACTTACCCTCAGTAACGTCGAAG
3 ←	CCACCGTAGAAGAATGGAGCACACTTACCCTCAGTAACGTCGAAG

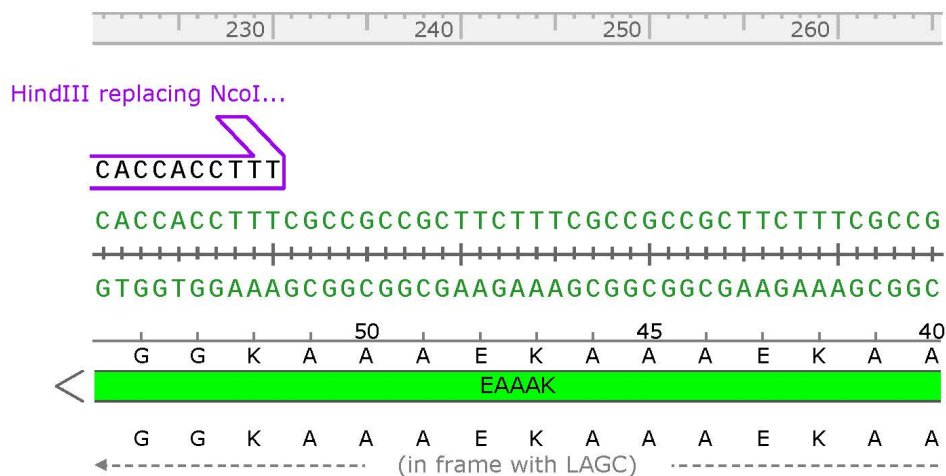


	TACCATCTAGAAATCATAGCTCTACATGGACCAGTCTCAGCTTGC
1 ←	TACCATCTAGAAATCATAGCTCTACATGGACCAGTCTCAGCTTGC
2 ←	TACCATCTAGAAATCATAGCTCTACATGGACCAGTCTCAGCTTGC
3 ←	TACCATCTAGAAATCATAGCTCTACATGGACCAGTCTCAGCTTGC

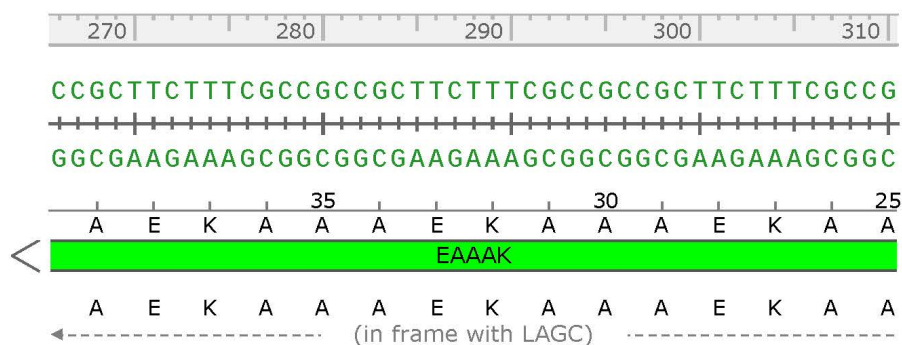
Final Clone Version 2.1\_AMRI\_alignment.dna (Circular / 5754 bp)



Final Clone Version 2.1\_AMRI\_alignment.dna (Circular / 5754 bp)

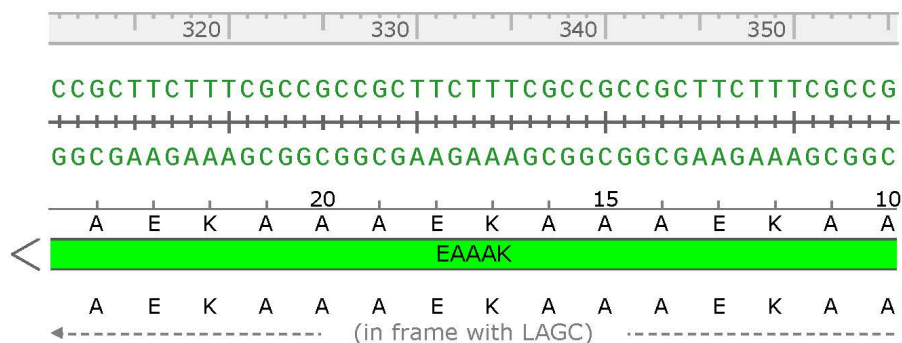


	CACCACCTTTTCGCCGCCGCTTCTTTTCGCCGCCGCTTCTTTTCGCCG
1	CACCACCTTTTCGCCGCCGCTTCTTTTCGCCGCCGCTTCTTTTCGCCG
2	CACCACCTTTTCGCCGCCGCTTCTTTTCGCCGCCGCTTCTTTTCGCCG
3	CACCACCTTTTCGCCGCCGCTTCTTTTCGCCGCCGCTTCTTTTCGCCG



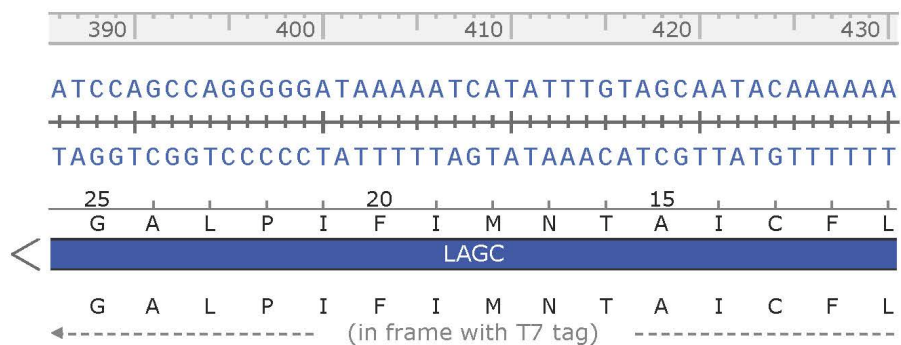
	CCGCTTCTTTTCGCCGCCGCTTCTTTTCGCCGCCGCTTCTTTTCGCCG
1	CCGCTTCTTTTCGCCGCCGCTTCTTTTCGCCGCCGCTTCTTTTCGCCG
2	CCGCTTCTTTTCGCCGCCGCTTCTTTTCGCCGCCGCTTCTTTTCGCCG
3	CCGCTTCTTTTCGCCGCCGCTTCTTTTCGCCGCCGCTTCTTTTCGCCG

Final Clone Version 2.1\_AMRI\_alignment.dna (Circular / 5754 bp)



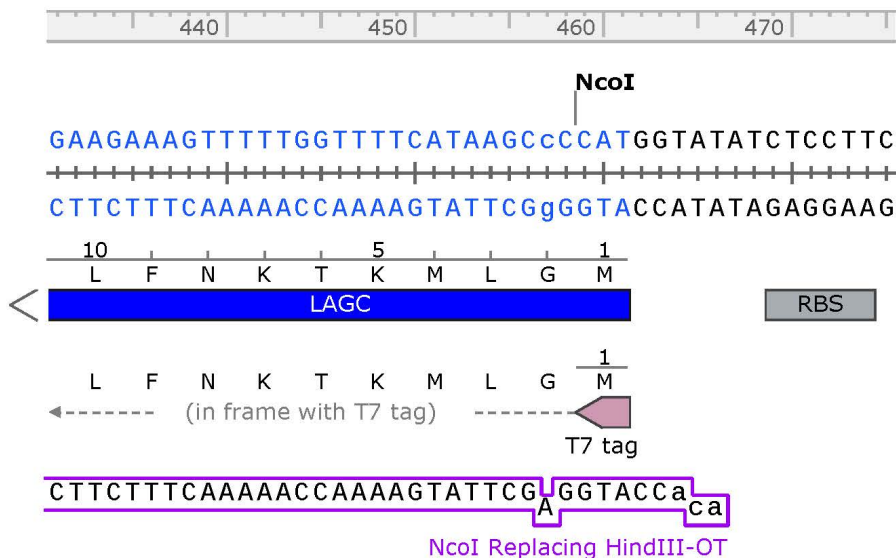


Final Clone Version 2.1\_AMRI\_alignment.dna (Circular / 5754 bp)

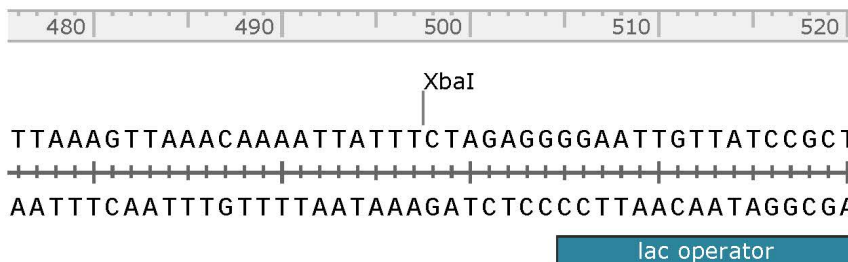


NcoI Replacing HindIII-OT

	ATCCAGCCAGGGGGATAAAAATCATATTTGTAGCAATACAAAAA
1	← ATCCAGCCAGGGGGATAAAAATCATATTTGTAGCAATACAAAAA
2	← ATCCAGCCAGGGGGATAAAAATCATATTTGTAGCAATACAAAAA
3	← ATCCAGCCAGGGGGATAAAAATCATATTTGTAGCAATACAAAAA



	GAAGAAAGTTTGGTTTTCATAAGCCCATGGTATATCTCCTTC
1 ←	GAAGAAAGTTTGGTTTTCATAAGCTCCATGGTATATCTCCTTC
2 ←	GAAGAAANTNNNTGGTTTTCATAAGCTCCATGGTATATCTCCTTC
3 ←	GAAGAAAGTTTGGTTTTCATAAGCTCCATGGTATNTCTCCTTC



	TTAAAGTTAAACAAAATTATTTCTAGAGGGGAATTGTTATCCGCT
1 ←	TTAAAGTTAANNAAAATTANTCTAGANNNA NNNNNNNNNNNN
2 ←	TTAAAGTTAANNNAAAATTANTCTANNNGNA NNNNNNNNNNNN
3 ←	TTAAAGTTAANCAAAATTNT

Final Clone Version 2.1\_AMRI\_alignment.dna (Circular / 5754 bp)

